Exploring long-term trends in hypoxia (oxygen depletion) in Western Gotland Basin, the Baltic Sea

Tianzhuo Liu

Dissertations in Geology at Lund University,
Master's thesis, no 295
(45 hp/ECTS credits)

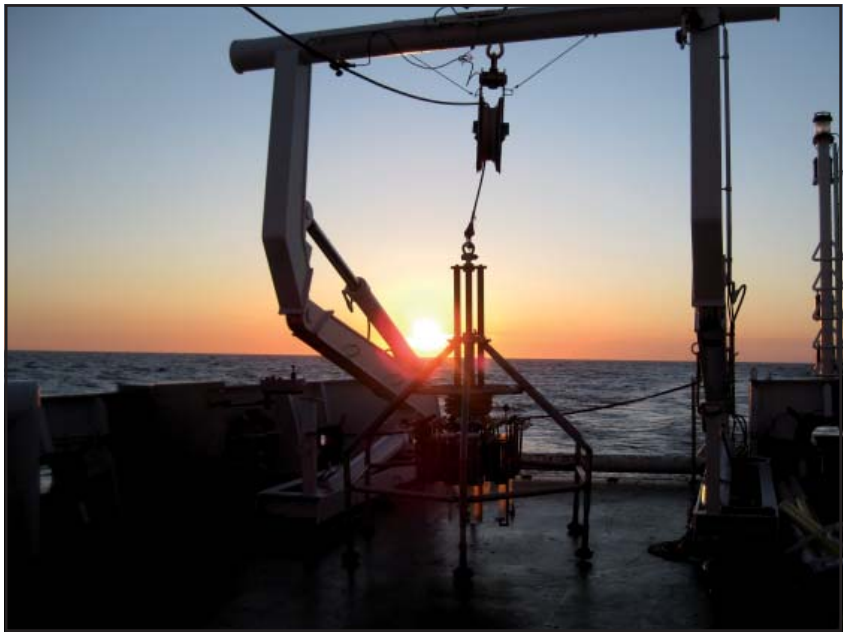

Department of Geology
Lund University
2012

Exploring long-term trends in hypoxia (oxygen depletion) in Western Gotland Basin, the Baltic Sea

Master's thesis

Tianzhuo Liu

Department of Earth and Ecosystem Sciences
Division of Geology
Lund University

2011

Contents

1 Introduction **1**
2 Study area **2**
2.1 The Baltic Sea 2
2.2 The history of the Baltic Sea 3
2.3 Western Gotland Basin 4
3 Methods **5**
3.1 Core collection, sediment description and subsampling 5
3.2 Mineral magnetic measurements 5
3.3 Loss on ignition measurements 6
3.4 Sediment geochronology 6
4 Results **7**
4.1 Mineral magnetic measurements 7
4.1.1 Magnetic susceptibility 7
4.1.2 SIRM 8
4.1.3 ARM 8
4.2 Loss on ignition 10
4.3 Chronology 10
4.3.1 Lead analysis 10
4.3.2 Radiocarbon dating 10
5 Discussions **11**
5.1 Identifying periods with hypoxia 11
5.2 Chronology 13
5.3 Origin of mineral magnetic signals 13
6 Conclusions **14**
7 Acknowledgements **15**
8 References **15**

Exploring long-term trends in hypoxia (oxygen depletion) in Western Gotland Basin, the Baltic Sea

Tianzhuo Liu

Liu, T. Z. (2011): Exploring long-term trends in hypoxia (oxygen depletion) in Western Gotland Basin, the Baltic Sea. *Dissertations in Geology at Lund University*, No. 295, 17 pp. 45 hp.

Abstract:

The Baltic Sea is suffering from bad ecosystem health due to strong impacts of anthropogenic activities. Since 1960, the hypoxic (< 2mg/l dissolved oxygen) area has expanded to c. 49 000 km^2, resulting in an amplified eutrophication, which severely threats the ecosystem of the Baltic Sea. The long-term trend in basin-wide hypoxia in the Baltic Sea is not fully understood. This study explores the temporal variability in long-term hypoxia in the Western Gotland Basin, a basin lacking good records of past hypoxia. Based on studies of one long sediment sequence in the Western Gotland Basin, the occurrence of hypoxia has been reconstructed for the last c. 8000 years. The sequence has been studied using various proxies for hypoxia and dated using accelerator mass spectrometry ^{14}C measurements (bulk sediment samples and a single macrofossil sample) and lead concentration and isotope ($^{206}Pb/^{207}Pb$) analysis. The hypoxic periods are characterized by laminated sediments, high carbon content and high magnetic concentrations. Mineral magnetic analyses show that single domain magnetite is the dominant ferrimagnetic mineral suggesting relative high abundance of magnetotactic bacteria during hypoxic periods. By correlation and synchronization with other sediment records from the Baltic Sea, this study demonstrates that open-sea hypoxia occurred basin-wide (western, eastern and northern Gotland Basins) at depth from c. 180 m-110 m during three major periods: (i) from 1960 to present (ii) from c. 1450±150 cal. yr BP to c. 650±150 cal. yr. BP and (iii) c. 5000-8000 cal. yr. BP. In contrast, a single radiocarbon date of a macrofossil remain (fish bone) suggests a younger age of the oldest laminated period i.e. centered around c. 4000 cal. yr. BP. The same date also suggests that the age of the Ancylus/Littorina transition is c. 6000 cal. yr. BP, which adds further insights to the discussion about the evolution of the "modern" Baltic Sea.

Keywords: Baltic Sea, hypoxia, lead analysis, lamination, mineral magnetism, loss on ignition, magnetotactic bacteria.

Tianzhuo Liu, Department of Earth and Ecosystem Sciences, Division of Geology, Lund University, Sölvegatan 12, SE -223 62 Lund, Sweden. E-mail: tianzhuo007@gmail.com

Exploring långsiktiga trender i hypoxi (syrebrist) i västra Gotlandsbassängen Östersjön

Tianzhuo Liu

Liu, T. Z., 2011: Exploring långsiktiga trender i hypoxi (syrebrist) i västra Gotlandsbassängen ÖstersjÖn. *Examensarbeten i geologi vid Lunds universitet*, Nr. 295, 17 sid. 45 hp.

Sammanfattning: Övergödningen är ett av de största hoten mot Östersjöns miljö. Den orsakar inte bara algblomning under sommarhalvåret utan även syrebrist (hypoxi). Utbredningen av syrefria bottnar i Östersjön har ökat fyrfaldigt sedan 1960-talet till följd av ökade utsläpp av näringsämnen, så som fosfor och kväve. Undersökningar av långa sedimentkärnor i Östersjön visar dock att dagens syrebrist inte är unik utan att det förekommit alternerande perioder med syrefria respektive syresatta bottenförhållanden de senaste ca 8000 åren. Tyvärr saknas det fortfarande kunskap om syrebristens utbredning i tid och rum, samt vilka orsaker som ligger bakom dessa variationer, vilket komplicerar förståelsen om hur Östersjöns ekosystem fungerar. Även om den förhöjda näringstillförseln är den direkta orsaken till dagens övergödning i Östersjön så är en ökad förståelse om syrebristens variationer nödvändig för att kunna driva en effektiv miljöförvaltning. I mitt magisterarbete har jag studerat en sedimentkärna från Västra Gotlandsbassängen - ett område som nästan helt saknar information om hypoxins variationer tillbaka i tiden. Syftet är att med hjälp av olika ”proxies” och dateringsmetoder d.v.s. kol-14 dateringar och blyanalyser (koncentration och isotopanalys $^{206}Pb/^{207}Pb$) rekonstruera hur syrebristen varierat tillbaka i tiden de senaste c. 8000 åren d.v.s. under Littorinahavet. Resultaten visar att perioder med syrebrist karakteriseras av laminerade sediment, en hög organisk kolhalt och en hög koncentration av magnetiska mineral. Analyserna visar att det dominerande magnetiska mineralet vid hypoxi utgörs av ett finkornig enkeldomänig ferrimagnetiskt mineral, troligtvis magnetit, producerat intracellulärt av bakterier s.k. magnetotaktiska bakterier (MTB). Genom korrelation och synkronisering med andra studier demonstrerar arbetet att storskalig (västra, norra och östra Gotlandsbassängerna) hypoxi har förekommit, på djup mellan ca. 180-110 m, under tre längre perioder: (i) sedan 1960, (ii) mellan ca 1450±150 och 650±150 kalenderår före nutid och (iii) mellan ca. 8000-5000 kalenderår före nutid. Intressant är att en kol-14 datering baserat på makrofossilrester (fiskben) demonstrerar att den nedre (äldre) perioden med hypoxi är mycket yngre (centrerad kring ca. 4000 kalenderår före nutid) än vad de flesta andra studier, och de åldrar som är baserade på kol-14 dateringar av sedimentbulkprover, visar. Samma datering föreslår även att övergången från Ancylussjön till Littorinahavet skedde för ca. 6000 kalenderår före nutid, vilket ytterligare spär på diskussion om när den ”moderna” Östersjön bildades.

Nyckelord: Östersjön, hypoxi, bly analys, laminering, mineral magnetism, glödgningsförlust, magnetotactic bakterier.

Tianzhuo Liu, Institutionen för geo– och ekosystemvetenskaper, Enheten för geologi, Lunds Universitet, Sölvegatan 12, 223 62 Lund, Sverige. E-post: tianzhuo007@gmail.com

1 Introduction

The modern Baltic Sea is a semi-enclosed brackish water body, suggested to have formed 8500 to 8000 years ago (Björck et al., 2008). It has an area of 412 560 km^2, containing three major basins: the Bothnian Bay, the Bothnian Sea and the Baltic Proper (Fig. 1A). Since 1960, increased human development has lead to a bad ecological environment in the Baltic Sea, especially the spread of hypoxia, which threatens the aquatic organisms.

Hypoxia, defined as <2 mg/l dissolved oxygen (DO), is a term first used by physiologists to describe the lack of necessary oxygen for aerobic respiring organisms in the bottom water (benthos). The hypoxia not only causes severe ecosystem disturbances (Diaz and Rosenberg, 1995), but also alters nutrient biogeochemical cycles (Vahtera et al., 2007).

One main reason for hypoxia is eutrophication. Eutrophication is the "bloom" or great increase of phytoplankton in the water body due to overloading with waterborne and airborne nutrients, such as nitrogen (N) and phosphorous (P). When the dense population of phytoplankton dies, they fall to the bottom where decomposition processes consume oxygen and cause reduced DO levels. Another reason for hypoxia is the vertical stratification of the water column due to the strong salinity gradient (or the presence of a strong halocline). The halocline reduces the vertical exchange of oxygen from the upper to the lower water masses resulting in a short supply of oxygen to the bottom waters.

Widespread hypoxia has become a globally significant problem with over 400 reported sites suffering from its effects (Diaz and Rosenberg, 2008). In the Baltic Sea, the hypoxic zone has increased four times since 1960 (Jonsson et al., 1990) and currently covers ca. 49 000 km^2 (Conley et al., 2009; Fig. 1B). The increase of hypoxia results in a high concentration of P in the water column, which is released from the sediments due to the reduced environment. This release results in a low N/P ratio in the surface water during summer, which favors the cyanobacteria, thereby amplifying eutrophication (Conley et al., 2002).

The geological records (Zillén et al., 2008) show that hypoxia has occurred several times during the Holocene, which means that hypoxia is not just a modern phenomena. Zillén et al. (2008) demonstrated that there are three major periods of hypoxia recorded in the sediments during the last 8000 years. These periods coincide with Holocene Thermal Maximum (HTM; 9000-5000 cal. yr BP), the Medieval Climate Optimum (MCO; AD 800-1200) and the general climate warming during most of the 20th century and the start of the 21st centuries AD (Fig. 2).

Apart from the climate impact, human activity may have played an important role in the development of hypoxia over the past two millennia (Zillén and Conley, 2010). Population dynamics have been suggested to be one of the main reasons. Data show that a doubling of the human population (from c. 4.6 to 9.5 million) occurred during the early-Medieval expansion in the Baltic Sea drainage area (Zillén and Conley, 2010). During this expansion, a massive reclamation of land occurred, which significantly increased the release of nutrients from the cultivated soil (Zillén and Conley, 2010). At the same time, technology innovations, such as the "modern" plow developed.

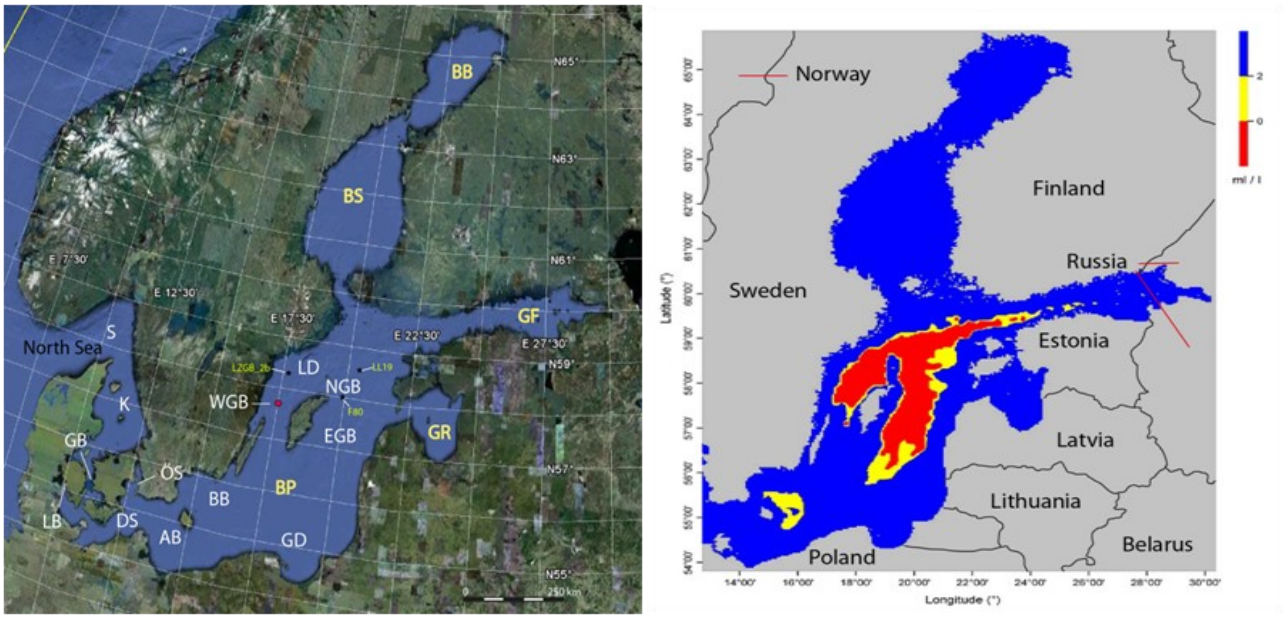

A B

Fig. 1. (A) Baltic Sea with major basin in yellow (BP=Baltic Proper, GR=Gulf of Riga, GF=Gulf of Finland, BB=Bothnian Bay, BS=Bothnian Sea), sub-basin and outlet in white (AB=Arkona Basin, BB=Bornholm Basin, GD=Gdansk Deep, WGB=West Gotland Basin, EGB=East Gotland Basin, NGB=North Gotland Basin, LD=Landsort Deep, DS=Darss Sill, K=Kattegat and S=Skagerrak, LB=Little Belt, GB=Great Belt, ÖS=Öresund Strait). (B) The modern distribution of hypoxia in the Baltic Sea (data obtain during a research cruise with R/V Aranda in 2008).

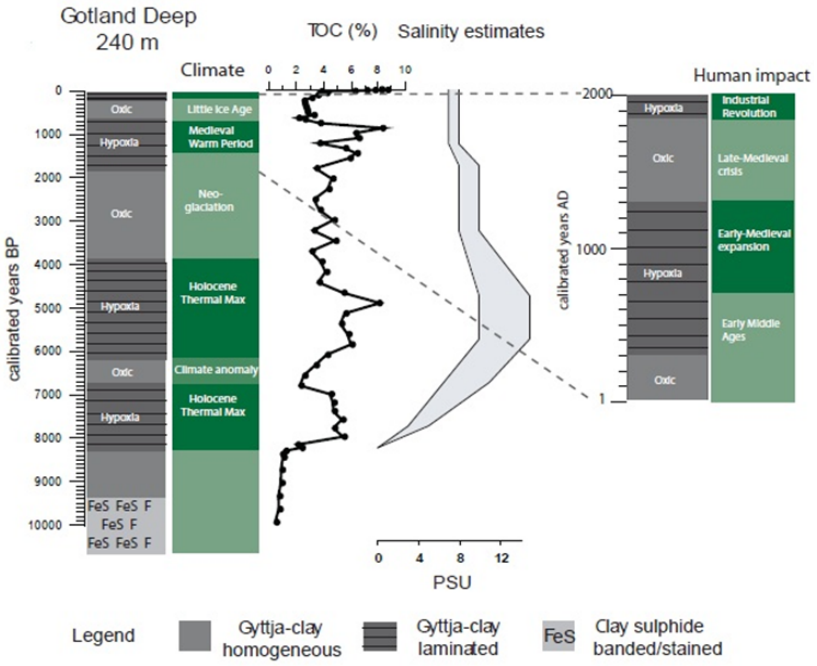

Fig. 2. Figure shows the occurrence of laminated sediments, total organic carbon content (TOC) and salinity estimates, plotted against a calendar year timescale, based on a compilation of sediment records from the Baltic Proper (Zillén et al., 2008) and a comparison to anthropogenic expansion and contraction phases in the same sediment records (Zillén and Conley., 2010).

Plowing increased the nutrient transport from the land to surface water bodies (Whitmore et al., 1992) and to the sea. For example, paleoecological studies show that the nutrient status of lakes in northern Europe has increased from Medieval time to the present (Renberg et al., 2001; Bradshaw et al., 2005).

It has been suggested that the occurrence of hypoxia in the early Holocene (c. 8000-4000 cal. yr BP) was caused by climate changes coupled with morphological changes in the depths of sills in the Baltic basin, while in the late Holocene there may have been an interaction between human and climate forcings (Zillén et al., 2008; Zillén and Conley, 2010).

To estimate to what degree human activity has altered the bottom water oxygen conditions in the Baltic Sea and to predict how projected climate changes may affect the spatial extent of hypoxia in the future, a detailed knowledge of the long-term natural variability of hypoxia is required. Instrumental records of oxygen concentrations are too short (< 100 years) and mostly fall within the period of intense human impact on natural conditions. Information on earlier periods can thus be obtained from environmental proxies.

Most previous studies using proxy records of hypoxia have focused on the eastern and northern Baltic Proper (eastern and northern Gotland Basin), and little work has been done in the western Baltic Proper (Western Gotland Basin WGB). One way to detect hypoxia is by identifying the occurrence of laminated sediments. These sediments can only be formed and preserved during specific conditions, which is a condition without bioturbation (vertical mixing) of sediments by benthic macrofauna. Laminated sediments have been frequently reported in the Baltic Proper (Zillén et al., 2008), but only a few within the WGB (of which the majority are located in the relatively isolated and deep Landsort Deep Basin). There are, therefore, significant gaps in our knowledge regarding the long-term spatial and temporal extent of hypoxia, which prevent an integrated understanding of the underlying mechanisms and system-wide response to external forcing.

The overall aim of this study is to increase our knowledge of the temporal and spatial distribution of hypoxia in the Baltic Sea during the majority of the Holocene. Specific aims of the present study are:

- To identify periods of hypoxia (laminated sediments) in the WGB using geological proxy-data.
- To obtain absolute ages for the time of formation of the different layers of laminated sediments.
- To correlate and synchronize periods of hypoxia in WGB with similar records in the Baltic Proper, and to give further insight on the driving mechanisms for open-sea hypoxia in the Baltic Sea.
- To study the mineral magnetic properties associated with hypoxia.

2 Study area

2.1 The Baltic Sea

The Baltic Proper can be sub-divided into the Gulf of Finland, the Gulf of Riga, and several basins, such as the Arkona Basin, Bornholm Basin, Gdansk Deep, West Gotland Basin, East Gotland Basin, North Gotland Basin, Landsort Deep, Kattegat and Skagerrak (Fig. 1A). Three outlets/inlets, the Little Belt, the Great Belt and Öresund Strait, are located in the southwest part of the Baltic.

The drainage area is about 1.6 million km^2, which is c. 4 times larger than the sea itself, and about 440 km^3 of freshwater per year drains into the basin. Additional 225 km^3 water originates as direct precipitation, with 185 km^3 of water removed by evaporation, resulting in a positive water budget for the Baltic Sea. Large water exchange between the North Sea and the Baltic Sea via the narrow and shallow belts and straits

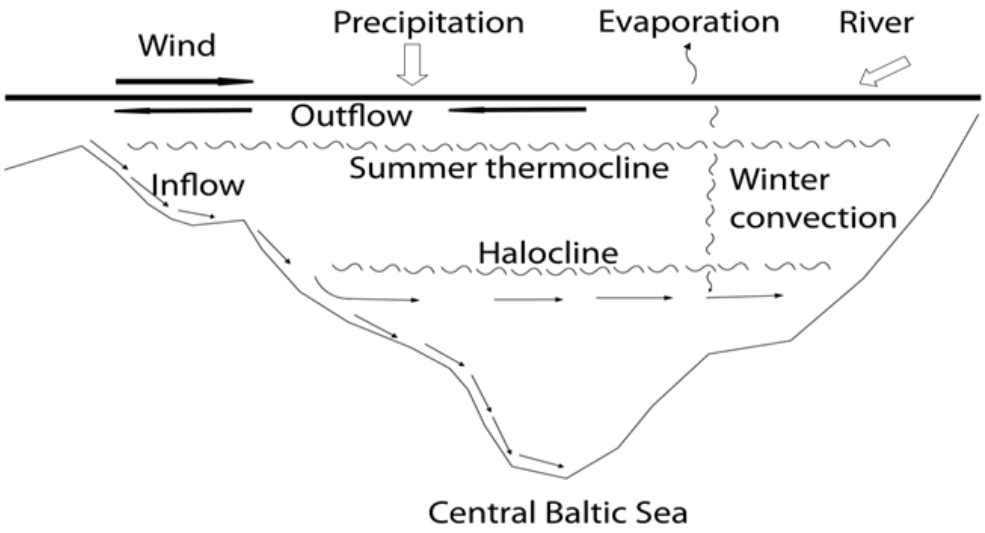

Fig. 3. Schematic picture of the water balance of the Baltic Sea, the water exchange with the North Sea (adapted from Lass and Matthäus, 2006).

occurs episodically and depends on the meteorological and oceanographic conditions. According to Matthäus et al. (2008) there are two types of inflows, major inflows occur when a period of easterly wind (one or two months, most commonly in September and October) creates a low sea level and followed by several weeks of a strong westerly winds (Schinke, 1996; Schinke and Matthäus, 1998). The other type is baroclinic summer inflow (exclusively fed by the Great Belt-Darss Sill gateway), which occurs after long lasting calm weather in the late summer or early autumn due to the baroclinic pressure gradients, especially horizontal salinity difference, and results in the spread of warm and saline water to the eastern Gotland Basin (Feistel et al., 2003c, 2004a). The saline inflow and the freshwater input yield in a salinity gradient where the surface salinity is c. 8-10 in the southern Baltic, c. 7-8 in the Baltic Proper and c. 3-5 in the Gulf of Finland, Bothnian Sea and Bothnian Bay (Matthäus, 2006).

The saline and oxygenated water from the North Sea is denser and heavier, so it flows along the bottom into the Baltic Proper, and a permanent vertical stratification of the water column is formed due to the salinity gradient (Fig. 3). The water column consists of two water masses, an upper brackish water mass and a deeper more saline water mass, with salinities of c. 7-8 and 11-13, respectively. The halocline is formed at the transition zone between these water masses, which inhibits vertical mixing and transfers the oxygen rich surface water to the bottom (Matthäus and Schinke, 1999). The depth of halocline is c. 30 m in the Arkona Basin, 60 m in the Bornholm Basin, 80 m in the Gotland Basin and the Landsort Deep (Matthäus, 2006).

2.2 The history of the Baltic Sea

According to the traditional late Quaternary history, the Baltic Sea has been divided into four main stages (Fig. 4), i.e. the Baltic Ice Lake, the Yoldia Sea, the Ancylus Lake and the Littorina Sea, which represent either brackish conditions with marine connections or isolated freshwater lake conditions (Björck, 1995).

When the final advance of the ice sheet ended (c. 17 000-16 000 cal. yr. BP), a proglacial lake formed in front of the receding ice sheet, which is the onset of the Baltic Ice Lake (Fig. 4a). Land uplift resulted in a transgression in the southern Baltic and a regression in the northern Baltic, and the Öresund area was eroded to its present level (Björck, 2008). This stage lasted until the end of Younger Dryas (c. 11 700-11 600 cal. yr. BP), when the connection between the North Sea and the Baltic Ice Lake, through the Mt. Billingen channel was formed and broadened, which allowed the saline water to penetrate (Andrén et al., 1999) and formed the first brackish phase: the Yoldia Sea stage (Fig. 4b).

With continued land uplift, the straits in Mt. Billingen became shallower and narrower, and finally closed. Due to the large freshwater input from glacial melting and precipitation, the Baltic water became fresh again. This fresh water phase was called the Ancylus Lake (around 10 700 cal. yr. BP; Fig. 4c) based on the diatom assemblage (Lemke, 1998). A transgression occurred in southern Baltic since the uplift here was slower than the water level rise, while a regression occurred in the northern Baltic. This tilting effect was considered as the beginning of the Ancylus Lake transgression (Björck, 2008).

The Ancylus transgression lasted for c. 500 years and ended abruptly by a sudden lowering of 10 m of the Ancylus water level, probably caused by erosion in Darss Sill (Fig. 1A). The transition between the Ancylus Lake stage and the following Littorina Sea stage is characterized by increasing marine influence. This influence has been dated to c. 9000 cal. yr. BP in Mecklenburg Bay. However, Andren et al. (2000) and Berglund et al. (2005) showed that marine waters already influenced the Bornholm Basin occasionally at c. 9800 cal. yr. BP. The beginning of the full Littorina Sea stage is usually defined as the large rapid expansion of saline water in the Baltic basin around c. 8500 cal. yr. BP (Björck, 2008; Fig. 4d). However, the age

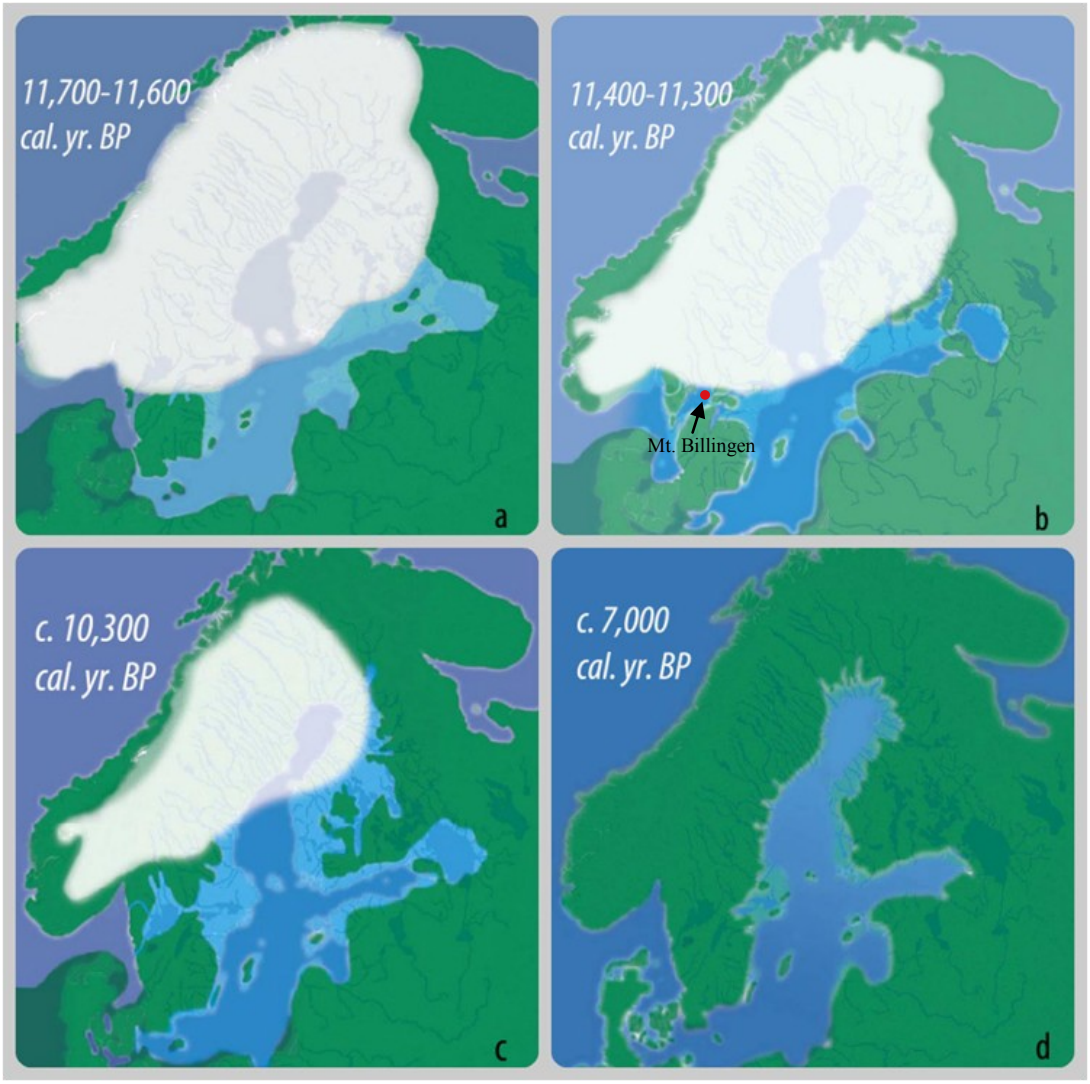

Fig. 4. The configuration of the Baltic area during the last deglaciation from Andrén (2003a,b,c; 2004). a. prior to the final drainage of the Baltic Ice Lake stage; b. the start of a short saline phase in the Yoldia Sea stage; c. the culmination of the Ancylus Lake stage; d. the start of the Littorina Sea stage.

of the A/L transition is still highly debated.

The following 2500-3000 years, the most significant Littorina transgression sets in, caused by the sudden collapse of Antarctic Ice Sheet and Laurentide Ice Sheet. Around c. 6000 cal. yr. BP, the salinity peaked even though some small transgressions still existed until c. 5000 cal. yr. BP.

The influx of saline water during the Littorina Sea stage changed the environment resulting in a change of the biological composition. For example, a majority of new species which favor the marine environment were present in the Baltic Sea at this time, consequently, abundant organic matters were produced and preserved in the sediments. Moreover, a permanent halocline was formed between the two water masses and subsequently, hypoxic conditions were formed in the bottom waters, demonstrated by the deposition of laminated sediments (Zillén and Conley, 2010; Fig. 2). The release of P from the sediments enhanced the cyanobacteria population, which probably also sustained the hypoxic condition (Bianchi et al., 2000).

2.3 Western Gotland Basin

The Western Gotland Basin (WGB) is defined as the area stretching from the southern Stockholm archipelago in the north to the city of Karlskrona in the south and reaching to the island of Gotland in the east (Håkansson et al., 2005). The basin includes one of the deepest parts of the Baltic i.e. Landsort Deep (460 m deep), and several shallow bank areas in the south which prevent deep water from penetrating into the WGB from the south. In addition, the deep, saline water has to enter from the north. However, this deepwater renewal only occurs during major saltwater inflows (Håkansson et al., 2005). Thus, the condition below the halocline is usually hypoxic or even anoxic (oxygen free). The summer surface water temperature at WGB is 18.0-19.7°C (Szaron, 2001), and the salinity in winter surface water is about 7 while below the halocline (80 m) is around 9 (Axe, 2004). The sediments consist mainly of glacial and postglacial clays. Also till clay, postglacial silt and sedimentary bedrock are common in the WGB (Fig. 5).

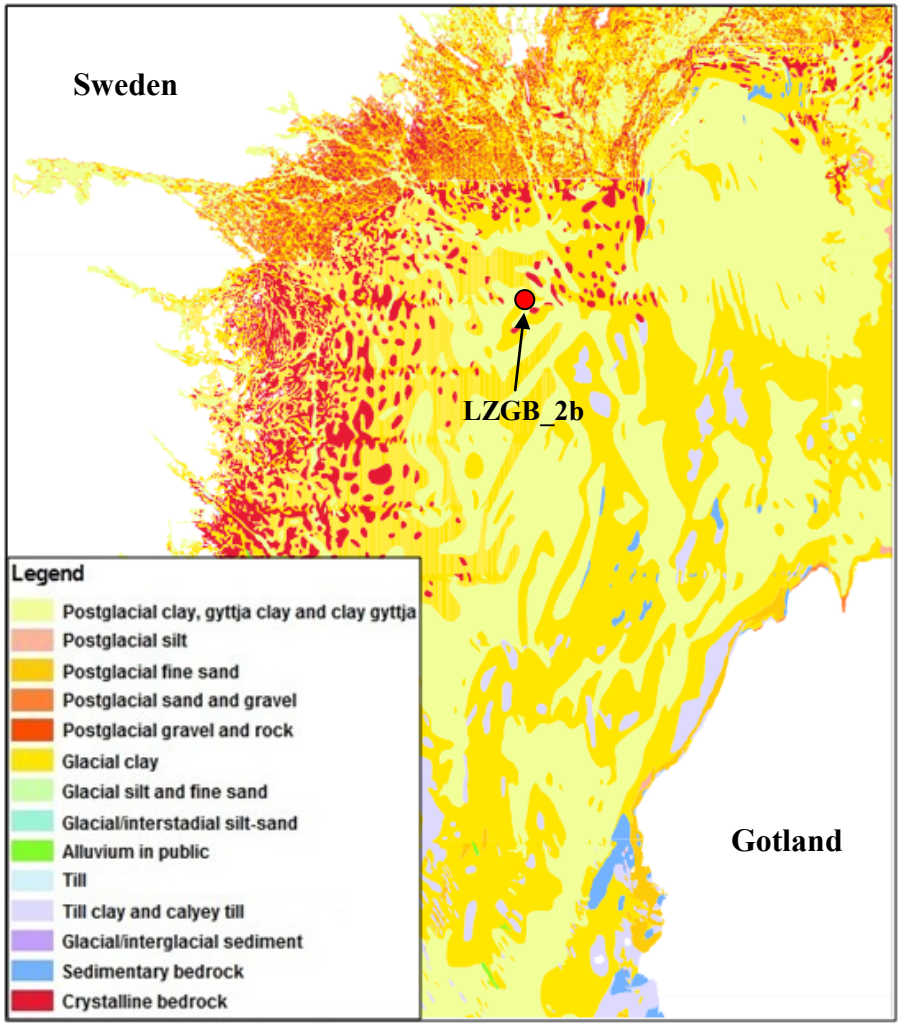

Fig. 5. Geological map of west Gotland Basin (data from the Geological Survey of Sweden)

3 Methods

3.1 Core collection and subsampling:

The sediment core was collected at the location approximately 58° 21'31.62" N, 17° 49'51.72" E (red circle; Fig. 5), in an area dominated by postglacial gyttja clay, during a research cruise with r/v Heincke in the summer of 2010 in WGB, and consists of a gravity core LZGB_2b (389.5 cm long) and a multicore (LZGB2, 41 cm long) from 109.5 m water depth. Sediment description was performed, using visual inspection to identify laminations and colors, and a standard ruler to measure the length of each interval.

The gravity core was split longitudinally into 2 parts, one for sediment description and subsampling, and the other for archive. Standard sized palaeomagnetic sampling cubes (2.2 x 2.2 x 2.2 cm external dimensions) were filled up with sediments at a resolution of 1 cm. The residual sediment were sliced in the same resolution and kept in plastic boxes. The multicore was sliced on-board at 1 cm resolution and put into plastic bags. In the laboratory, they were subsampled at the same resolution and put into standard cubes.

3.2 Mineral magnetic measurements:

Mineral magnetic properties can give indications of what kind of material is present in the sediment sequence and also its provenance. For example, magnetic susceptibility (χ) can be used for detecting the concentration of magnetic minerals, and other parameters can be combined to indicate magnetic grain size (table 1).

Magnetic domains can be spontaneously magnetized in only one direction. The presence of one or more magnetic domains determines the magnetic hysteresis characteristics of ferrimagnetic minerals. The size and shape of the magnetic grains can also affect the behavior of the magnetic domains (Walden et al., 1999) and each domain is separated from the next by a domain wall. Ferrimagnetic crystals can be divided into three types: single-domain (SD), pseudo-single domain (PSD) and multi-domain (MD) (Thompson and Oldfield, 1986).

The SD grains are the smallest remanence carrying grains of any magnetic material, while the MD grains are larger grains that have domains separated by domain walls. The interaction between domain walls is responsible for the lower magnetic stability (coercity) of MD grains compared to SD grains. PSD grains are

Table 1. Compilation of mineral magnetic parameters and their interpretations (applicable to magnetite)

ABBREVIATION	DESCRIPTION	UNITS	INTERPRETATION
χ	Mass-specific magnetic susceptibility	m^3kg^{-1}	A reflection of ferrimagnetic mineral concentration. An indicator of the mix of ferrimagnetic, paramagnetic and diamagnetic minerals.
χ_{ARM}	Susceptibility of ARM	m^3kg^{-1}	ARM normalized by the bias field: extremely selective of finer ferrimagnetic grains. A concentration-dependent parameter.
ARM	Anhysteretic remanent magnetisation	Am^2kg^{-1}	Especially sensitive to proportion of fine single-domain (SD) ferrimagnetic minerals.
SIRM	Saturation isothermal remanence magnetisation	Am^2kg^{-1}	A high field induced magnetization (usually 1T). Generally a measure of selective of ferrimagnetic concentration in the mineral assemblage.
χ_{ARM}/χ			The ratio indicates an inverse proportion to the ferrimagnetic grain-size: small (SD) grains tend to show high values.
χ_{ARM}/SIRM		$A^{-1}m$	Indicates the variation in magnetic grain size. Unaffected by dia- and paramagnetic content. It's more size-sensitive within the MD range (Maher 1999).
SIRM/χ		Am^{-1}	A ferrimagnetic grain size measurement, but it can be varied by the para- and diamagnetic minerals when the ferrimagnetic concentration is low. Higher (lower) values indicate SD (MD) grains for those samples dominated by magnetite.

intermediate in size and coercity (Walden et al., 1999).

Different mineral magnetic measurements have been used during the study. A compilation of magnetic parameters and their interpretations are shown in table 1. All the measurements were carried out on the discrete palaeomagnetic samples.

To measure the volume magnetic susceptibility (κ) on the split core surfaces, a Bartington Instruments MS2E1 surface-scanning sensor was used at a resolution of 5 mm, combined with a TAMISCAN conveyor. Mass-specific susceptibility (χ) was measured by Geofyzica Brno Kappabridge KLY-2 after the core was subsampled. It reflects the concentration of ferrimagnetic minerals in the sample.

Anhysteretic remanent magnetization (ARM) and Saturation isothermal remanent magnetization (SIRM) measurements were performed subsequently. ARM, was induced in a decreasing alternating field (AF)(100 -0mT) in the presence of a direct field (DC) bias field of 0.05 mT using the coils of a 2G-Enterprises model 755-SQUID magnetometer.

Saturation isothermal remanence magnetisation (SIRM), was induced with a DC field at 1T using a Redcliffe 700 BSM pulse magnetizer. Both of them (ARM and SIRM) were measured with a Molspin Minispin magnetometer.

3.3 Loss on ignition measurements:

Loss on ignition is a common and widely used method to estimate the organic and carbonate content of sediments (Dean, 1974; Bengtsson and Enell, 1986). The samples, which weighed approximately 0.5 g each, have been selected from both the long gravity core and the multi-core at a resolution of 5 cm and 2 cm, respectively. The samples were kept in an oven at 105°C for more than 12 hours, then placed in a furnace at 550 °C for 4 hours to combust the organic materials. The weight loss during the process is measured by weighing the samples before and after heating. A desiccator was used during cooling (Heiri et al. 2001).

3.4 Sediment geochronology:

The chronology of the core is based on AMS ^{14}C measurement and total lead concentration and isotopic ratio of Pb^{206}/Pb^{207}.

The radiocarbon dating is a radiometric dating using ^{14}C to estimate the age of carbon-bearing materials up a maximum of about 58 000 to 62 000 years (Plastino et al., 2001). ^{14}C is widely spread in the atmosphere, and the photosynthesis can fix a certain amount of ^{14}C into plants which approximately matches the level of this isotope in the atmosphere. When plants die or are consumed by other organisms, the ^{14}C fraction of this organic material declines at a constant rate, which is the decay rate of ^{14}C. Thus, comparing the remaining ^{14}C of the sample to the expected atmospheric ^{14}C allows estimating the sample's age (Lowe and Walker, 1997). AMS ^{14}C measurement was performed at the AMS Laboratory at Lund University. Six bulk sediment samples and one fish bone were analyzed, and the result was calibrated using OxCal. Version 4.1 with marine09 calibration curve (Bronk Ramsey, 2009).

Isotopic and total lead concentration analyses by a quadrapole ICP-MS following acid dissolution (EPA3052) were performed on 41 samples, comprising 1 to 2 cm thick intervals of the upper c. 160 cm of the sediment sequence. For extraction, 5 ml of water, 2 ml H_2O_2, 9 ml HNO_3, 3 ml HCl and 2 ml HF were added to approximately 500 mg of ground, freeze-dried and homogenized sediment, after which microwave digestion and filtering were carried out. 1 ml of

Table 2. Sediment description of multi-core (LZGB2).

DEPTH (cm)	FEATURES	COLOR	SEQUENCE
0-12	laminated gyttja clay	black and dark brown	M1
12-41	homogeneous gyttja clay	brownish	M2

Table 3. Sediment description of gravity core (LZGB2b).

DEPTH (cm)	FEATURES	COLOR	SEQUENCE
0-31	homogeneous gyttja clay	light gray	1
31-56	laminated gyttja clay, with 2 cm homogeneous gyttja clay layer at 51-53	black, grayish green and dark brown	2
56-86	homogeneous gyttja clay with poorly laminated and laminated gyttja clay layers at 72-78 and 83-86, respectively	Light gray, brownish, bluish-gray, dark gray	3
86-111.5	homogeneous gyttja clay	bluish-gray	4
111.5-120.5	poorly laminated gyttja clay	brownish and dark gray	5
120.5-161.5	homogeneous gyttja clay with 1 cm laminated layer at 132-133	bluish-gray	6
161.5-170.5	laminated gyttja clay	brownish and dark gray	7
170.5-198	homogeneous gyttja clay	bluish-gray	8
198-226	laminated gyttja clay with 2 thin homogeneous gyttja clay layers at 200-205,209-212	black, gray and bluish	9
226-250	laminated clay gyttja	black, grayish	10
250-285	laminated gyttja clay with homogeneous gyttja clay and laminated clay gyttja layers at 259-264 and 275-277,respectively. Poorly laminated gyttja clay at 279-285	black, gray, grayish, and bluish	11
285-315	homogeneous gyttja clay	blue, black, light gray	12
315-389.5	homogeneous clay	bluish-gray	13

sample was added to 8 ml of water and 1 ml of internal standard stock for total lead concentration analysis, while isotopic analysis required 1 ml of each sample to be added to 9 ml of water. The analyses were conducted on a Perkin Elmer Elan 6100 DRC Plus ICP Mass Spectrometer at Durham University (UK) Department of Geography, Science Laboratories. Certified reference materials (SRM 981) were used for isotopic analysis (Zillén et al., 2011).

4 Results

The sediment sequence consists of a gravity core LZGB_2b (389.5 cm long) and a multi-core LZGB2 (41 cm long). The sediment descriptions are shown in table 2 and 3.

4.1 Mineral magnetic measurements

4.1.1 Magnetic susceptibility

χ, ARM, SIRM were performed on all the discrete samples (1 cm resolution) from the gravity core and multi-core (Fig. 6 and 7). The start of Ancylus Lake/ Littorina Sea (A/L) transition is characterized by the first increase in LOI, due to increased organic productivity and/or good organic preservation conditions. Another characterization is the decrease in SIRM, as the concentration of detrital minerals and greigite (a typical ferrimagnetic mineral in Ancylus Lake sediments) diminished. The distinct change can be identified in both of the curves at c. 315 cm (Fig. 6).

χ and SIRM were chosen for trying to identify the overlap between the gravity core and multi-core. No matching point or a similar trend could be identified in the χ and SIRM data (Fig. 6) and therefore, no overlap between the multi-core and gravity core has been confirmed.

The results of κ and χ reflect the presence of magnetic minerals and especially the concentration of ferrimagnetic minerals, such as magnetite. κ is widely used for correlations, because the measurement and the identification of magnetic minerals are faster and at a higher resolution (5 mm) than χ; χ is for more detailed analysis to i.e. calculate various ratios such as SIRM/χ and χ_{ARM}/χ. The highest values of κ and χ correlate to the sections with laminations (Fig. 6),

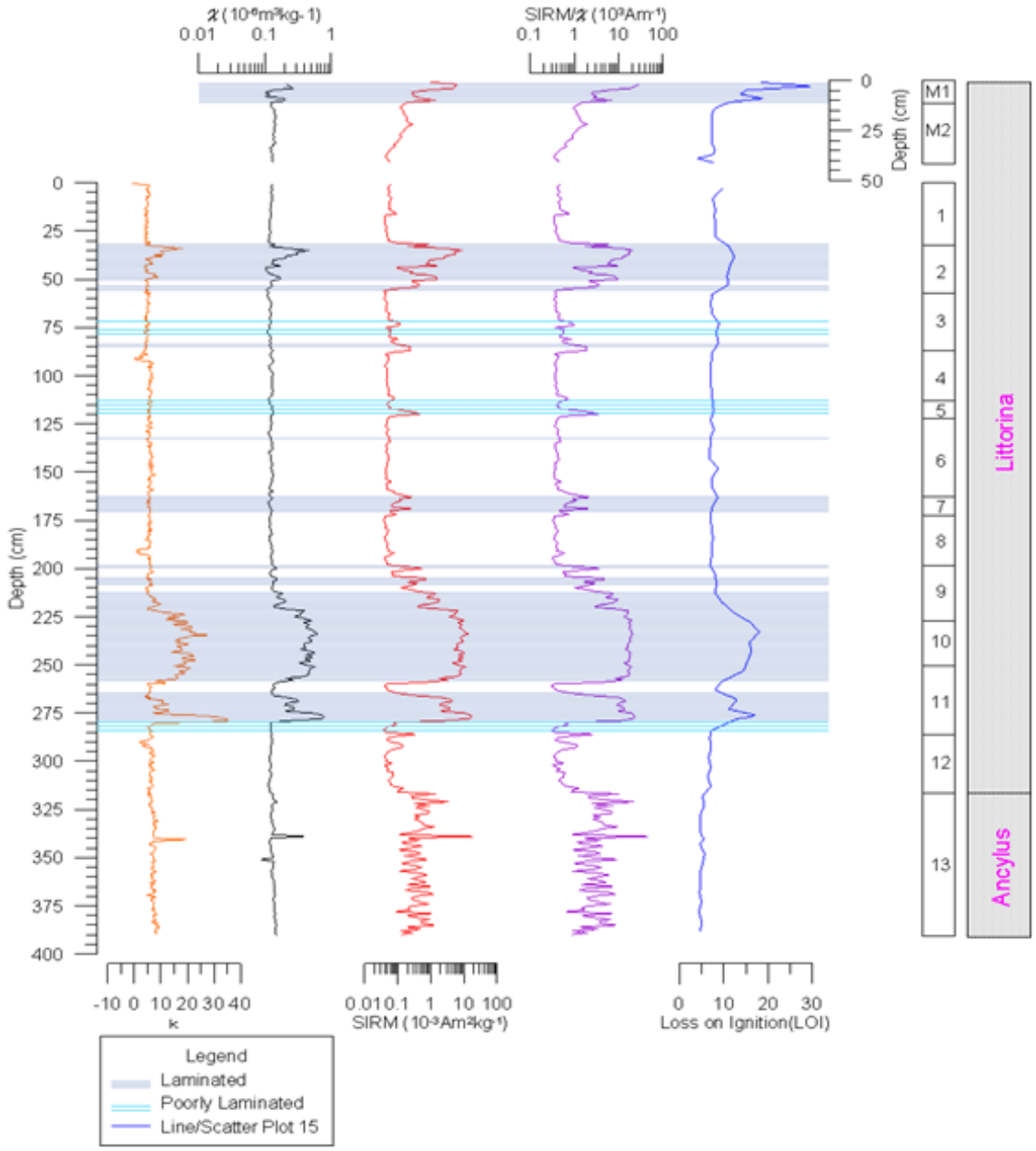

Fig. 6. Loss on ignition result and mineral magnetic parameters results of magnetic susceptibility, χ, SIRM and the ratio SIRM/χ.

indicating a higher concentration of ferrimagnetic minerals. High χ values occur at the depths of 198-285 cm and 31-56 cm in the gravity core and 0-12 in the multicore. The homogeneous parts of the sediment sequence are characterized by lower values (5-10 for κ and 0.1-0.2 * $10^{-6}$$m^3kg^{-1}$ for χ).

4.1.2 SIRM

SIRM and SIRM/χ show high values in the laminated-parts, corresponding to the trends in χ. Large changes between laminated and non-laminated can be identified in both curves (Fig. 6), which, according to table 1, indicates that the laminated parts are dominated by fine grained ferrimagnet. It is notable that there are small peaks (SIRM values rage between 0.1-1 * 10^{-3} Am^2kg^{-1}) in the poorly laminated intervals between 70 and 170 cm, probably due to the contribution of similar ferrimagnetic grains.

4.1.3 ARM

The ARM signals of many samples were below the sensitivity of the Molspin during measurements. Raw values below 2 * $10^{-3}$$Am^{-1}$ (relative to the calibration sample) were discarded because the signal to noise ratio is 10 and the lowest noise level is 0.2 * $10^{-3}$$Am^{-1}$. The results can only be interpreted when the ARM raw value are above 2 * $10^{-3}$$Am^{-1}$.

In Figure 7, the red dots represent reliable data, while the green dots represent discarded data. In general, reliable data are received from the laminated intervals where the concentration of ferrimagnetic minerals are high (as shown by high χ and SIRM values in figure 6). The high ARM values in the Ancylus clay probably reflect the presence of greigite.

The high χ_{ARM}/SIRM values in the homogeneous

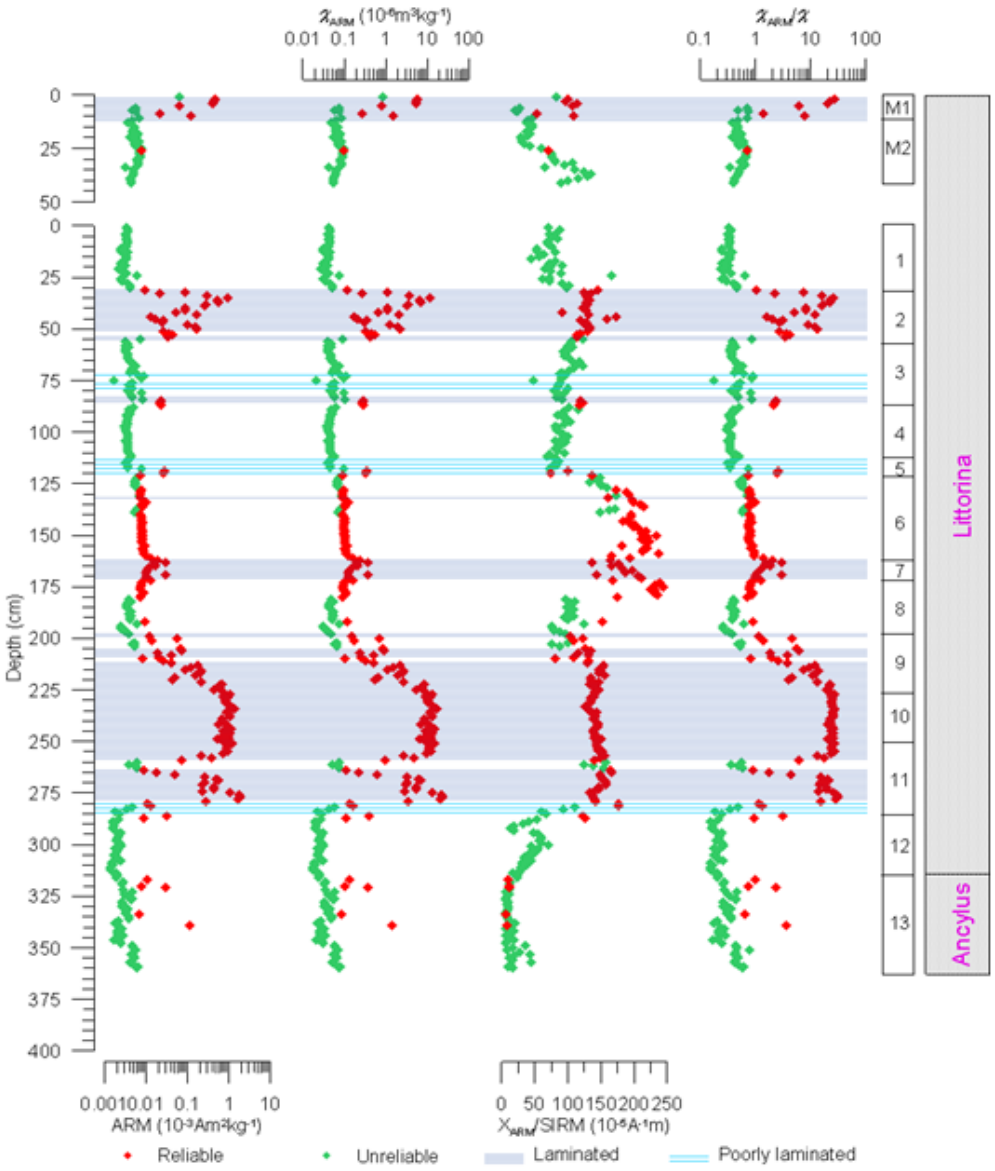

Fig. 7. A plot of the parameters of ARM, χ_{ARM}, χ_{ARM}/SIRM, χ_{ARM}/χ. Red samples represent reliable data, and green samples represent unreliable data.

part between 127 and 180 cm may be due to a measuring artifact. The raw data of ARM between 127 and 180 cm are approaching the background level of the Molspin and can result in a high χ_{ARM}/SIRM ratio.

ARM and χ_{ARM} are concentration-dependent parameters (table 1) and are particularly sensitive to the presence of SD magnetic grains. The ratios that indicate magnetic grain size (the χ_{ARM}/χ ratio and χ_{ARM}/SIRM ratio) indicate that SD grains cause the concentrations of magnetic minerals. χ was measured after drying (40 °C) and a plot of susceptibility loss (χ_{wet} - χ_{dry}) versus χ_{ARM}/SIRM is shown in figure 8.

Figure 8 indicates that many samples contain a material with χ_{ARM}/SIRM between the range of 120 and 160 * $10^{-5}A^{-1}m$, which alters upon drying. These samples correspond to the samples distributed in the laminations (Fig. 7). The figure shows that the material lost during storage has a narrow χ_{ARM}/SIRM range, characteristic of fine-grained SD magnetite (table 1).

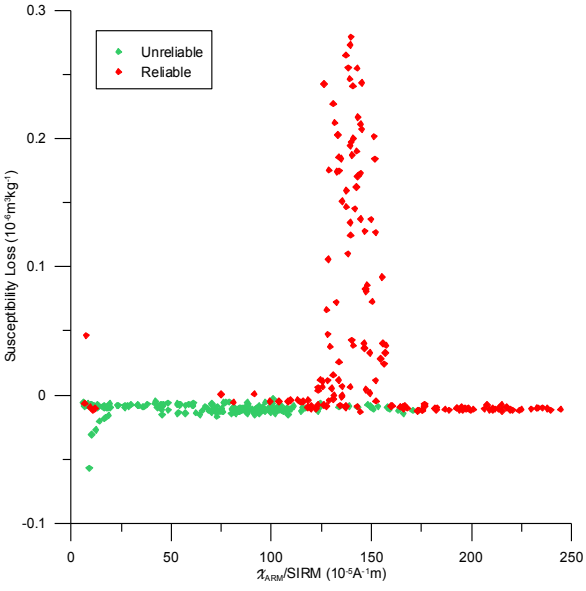

Fig. 8. A plot of susceptibility loss vs χ_{ARM}/SIRM

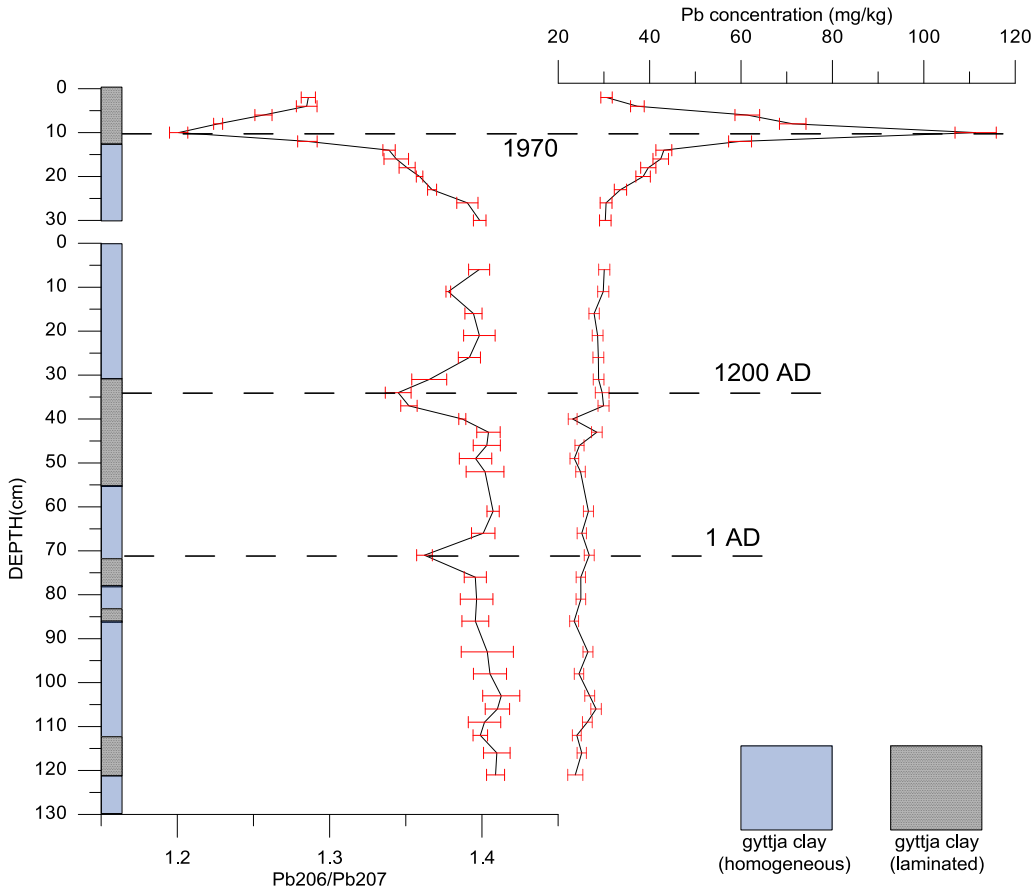

Fig. 9. The result of lead analysis in Pb concentration and ratio of Pb^{206}/Pb^{207}

4.2 Loss on ignition

Loss on ignition (LOI) ranges from 0 to 30. After estimating the organic carbon content (i.e. LOI * 0.4, Snowball et al., 2010), the sediments can be divided into three types i.e. clay (< 2% organic carbon content), gyttja clay (2-6% organic carbon content) and clay gyttja (6-20% organic carbon content).

The laminated parts are characterized by high LOI values, probably due to a high organic productivity and/or better preservation condition (low oxygen condition) during the formation of the laminated sediments.

4.3 Chronology

4.3.1 Lead analysis

The Pb concentrations and Pb206/Pb207 ratios are presented in figure 9. A distinct peak in Pb concentration occurs at a depth of 10 cm in the multi-core. In total, three major anomalies in the Pb206/Pb207 ratio have been identified, one at a depth of 10 cm in the multi-core (which correlates to the Pb-concentration peak in the same core) and the others are at the depths of 34 cm and 71 cm in the gravity core. The peak/troughs in both curves are characteristic of atmospheric lead pollution (Renberg et al., 2000).

Three major Pb-pollution isochrones have bee reported in terrestrial records in Europe (Renberg et al., 2000) and in the Baltic Sea (Zillén et al. 2011) i.e. the Roman peak (1AD), the Medieval peak (1200AD) and the 1970s peak. The peak/trough in the Pb-concentration and isotope ratio, respectively, in the multi-core is interpreted as the 1970s peak. The two largest isotope ratio anomalies in the gravity core (at 34 cm and 71 cm) are interpreted as the Medieval peak and Roman peak, respectively.

4.3.2 Radiocarbon dating

The sample depth (in gravity core) is from 31 to 286 cm (table 4), which covers approximately 6000 years (1900-7800 cal. yr. BP) based on calibrated ^{14}C ages. An age reversal occurs between c. 30-36 cm, probably due to that the dating materials are bulk sediment samples, which can be affected by the contribution of old redeposit organic materials.

Since the level of atmospheric ^{14}C is not constant (due to production changes and the carbon cycle), a calibration of ^{14}C ages is necessary to eliminate the impacts. However, due to the age reverse between 30-36 cm, a time/depth curve cannot be made by Oxcal., consequently, the ^{14}C ages were calibrated one by one.

The calibrated bulk ages are usually older than those based on analysis of macrofossil remains due to the additional mixture of older redeposit organic carbon materials (e.g. Roesslor et al., 2010). In order to test the age difference between the bulk ages and those based on analysis of macrofossil remains and Pb-dating, a plot of calibrated age/depth has been made,

Table 4. Coring device, location, water depth, radiocarbon ages and calibrated ages. The macrofossil (fish bone) sample has been weighted as 0.4 mg C

Core	Coring device	Latitude N	Longitude E	Water Depth (m b.s.l.)	Lab no	Sample (cm)	Dated material	Age ^{14}C BP	Cal. age BP (2σ range)
LZGB2b	Gravity core	58° 21'31.62"	17° 49'51.72"	109.5	LuS 9435	31-32	Bulk sample	2135 ± 50	1538-1884
LZGB2b	Gravity core	58° 21'31.62"	17° 49'51.72"	109.5	LuS 9437	35-36	Bulk sample	1950 ± 50	1340-1682
LZGB2b	Gravity core	58° 21'31.62"	17° 49'51.72"	109.5	LuS 9436	54-55	Bulk sample	3810 ± 50	3570-3950
LZGB2b	Gravity core	58° 21'31.62"	17° 49'51.72"	109.5	LuS 9440	214-215	Bulk sample	5005 ± 50	5137-5562
LZGB2b	Gravity core	58° 21'31.62"	17° 49'51.72"	109.5	LuS 9457	248-249	Fish bone	4215 ± 60	4080-4515
LZGB2b	Gravity core	58° 21'31.62"	17° 49'51.72"	109.5	LuS 9439	258-259	Bulk sample	6700 ± 55	7056-7400
LZGB2b	Gravity core	58° 21'31.62"	17° 49'51.72"	109.5	LuS 9438	285-286	Bulk sample	7775 ± 55	8060-8384

where the bulk ages and macrofossil and Pb ages are plotted separately (Fig. 10). The upper two Pb-age points represent the pollution start and the pollution trough in Pb^{206}/Pb^{207} ratio during the Medieval period, which correspond to the age of 1050±150 and 750±150 cal.yr.BP (Bränvall et al., 2001; Renberg et al., 2000), respectively. In core LZGB_2b, these two age points are at the depth of 43 and 34 cm. The isotope anomaly at 71 cm is interpreted as the Roman lead peak (Fig. 9). This peak is usually the less distinct peak in the European lead pollution record (Renberg et al., 2000; Zillen et al., 2011). However, if the sedimentary rate in the uppermost part of the sediment sequence is constant, the trough in Pb^{206}/Pb^{207} ratio at 71 cm corresponds to an age of c. 1 AD.

5 Discussion

5.1 Identifying periods with hypoxia

Both climate forcing and human impact can induce hypoxia (Zillén et al., 2008; Zillén and Conley, 2010). In this study, three major periods of hypoxia have been identified using environmental proxies such as, the presence of laminations, LOI and mineral magnetic properties. These periods have been dated using

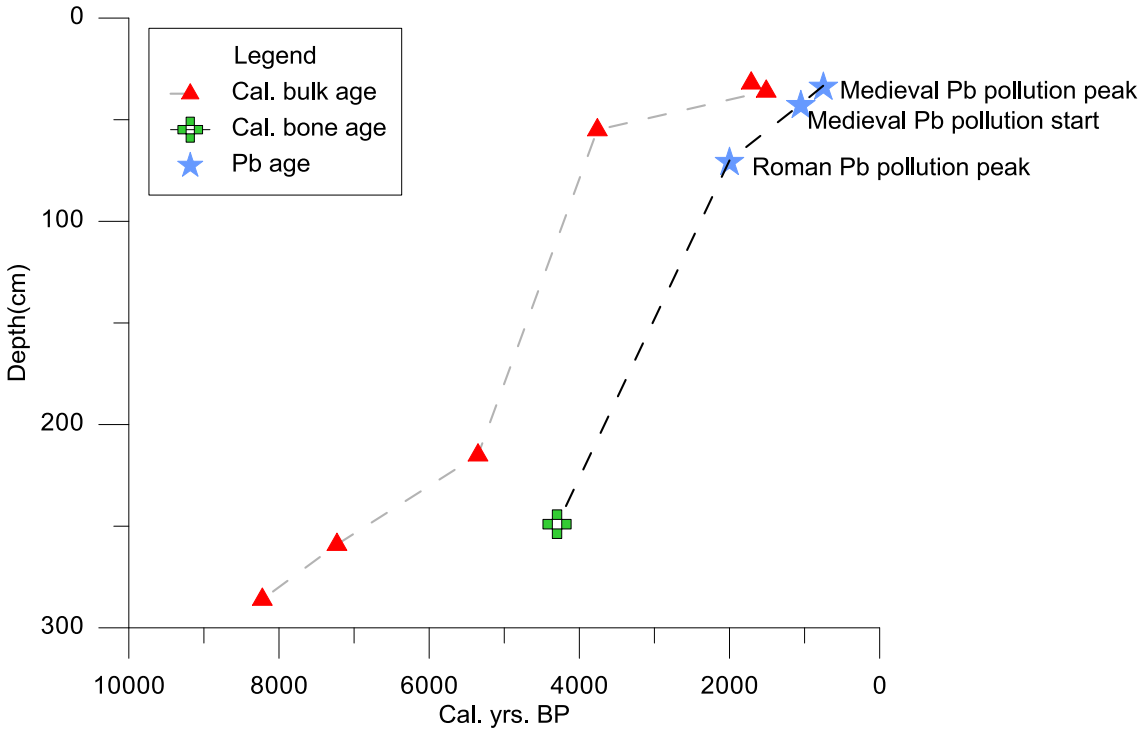

Fig. 10. A plot of calibrated bulk ages, calibrated bone age and Pb ages from Bränvall et al. (2011) vs depth.

radiocarbon measurements and lead concentration and isotope analysis, which correlate to HTM, MCO and the past period since 1960, similar to Zillén et al., (2008).

The three major periods of hypoxia (laminated sediments) are characterized by high LOI values and high mineral magnetic concentrations (Fig. 6). The first minor increase of LOI occurs at 315 cm (Fig. 6), which has been identified as the A/L transition, when the first saline water entered the Baltic Sea basin i.e. the Early (or Initial) Littorina Sea (c. 10 000–8500 cal. yr BP; Berglund et al., 2005). But a further rapid increase occurs at about 285 cm, corresponding to the first formation and preservation of laminated sediments. At this time, saline water flowed into the Baltic Sea: it not only completely changed the water condition i.e. the salinity and the concentration of dissolved oxygen, but also enhanced the organic productivity. This high LOI period correlates to the beginning of the full Littorina Sea stage (or Littorina Sea sensu stricto c. 8500–3000 cal. yr BP; Berglund et al., 2005) based on bulk radiocarbon dating (table 4). However, due to the large uncertainties associated with bulk radiocarbon dating of Baltic Sea sediments, the duration of the laminated period during the beginning of the Littorina Sea will be discussed in the next section (cf. Geochronology).

The second period of lamination occurs at 56 cm and ends at 31 cm, which correlates to MCO period based on the lead concentration and isotope analysis (Fig. 9). According to Bränvall et al. (2001), the start of decreasing in ratio Pb^{206}/Pb^{207} during medieval period is 1050±150 cal. yr. BP and the trough is 750±150 cal. yr. BP, which corresponds to the depth of 43 and 34 cm in gravity core, respectively, indicating a sedimentation rate of 0.33 mm/yr. If the rate was constant, the timing of medieval lamination is from c. 1450±150 to 650±150 cal. yr. BP.

The reason for hypoxia might be due to a combination of climate forcing and human impacts (Zillén et al., 2008; Zillén and Conley, 2010). Warm climate may increase primary productivity and anthropogenic development around the Baltic can increase the nutrient input to the sea. Consequently, eutrophication probably spread during this period and low oxygen conditions resulted in good sediment preservation conditions.

The youngest period with hypoxia is identified at 12-0 cm in the multi-core and correlates to the period since 1960 (based on the lead peak and calculated sedimentation rate) when human impacts (via the use of synthetic fertilizer) have accelerated.

In order to increase the knowledge about the temporal and spatial distribution of hypoxia in the past

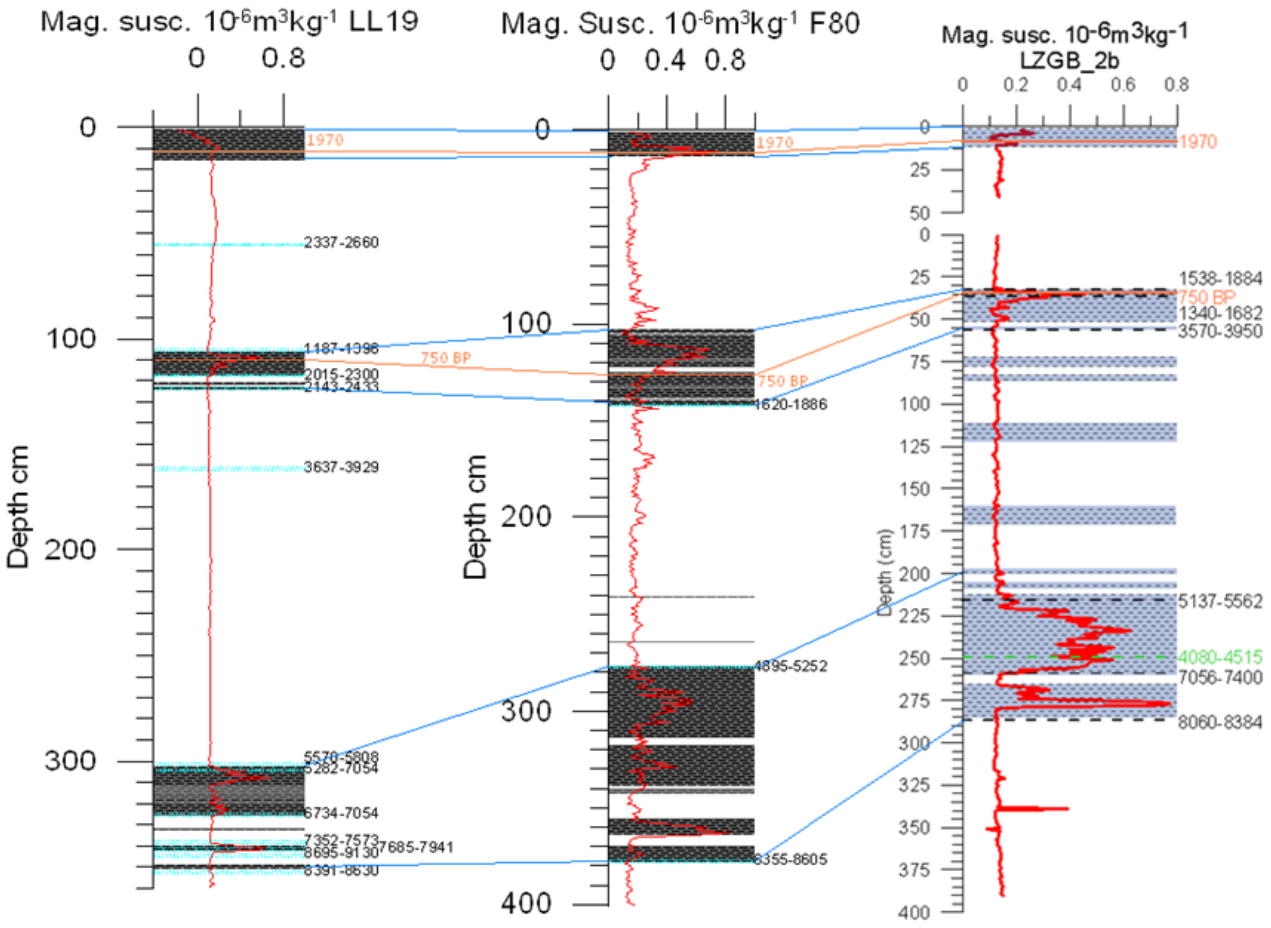

Fig. 11. Correlation of LL19, F80 (Reinholdsson et al. in prep; see Fig. 1A) and LZGB_2b, orange figures represent lead peak age (Zillén et al., 2011 and this study), green figure in LZGB_2b represents calibrated fish bone age and black figures are calibrated bulk ages.

a comparison with other studies with similar proxy and dating records as in this study (Reinholdsson et al., in prep; Zillén et al., 2011) has been made (Fig. 11).

The three major periods with laminated sediments in LZGB_2b (this study) correlates to similar periods in both LL19 (North Gotland basin, Fig. 1A, water depth 169 m) and F80 (East Gotland Basin, Fig. 1A, water depth 181 m), which are all characterized by high χ values. For the first time, lead isochrones from different sub-basins (i.e. western, northern and eastern Gotland basins) show that hypoxia occurred at the same time on a basin-wide scale (i.e. Baltic Proper) during the Medieval period. The lead isochrones also demonstrates that, at water depths shallower than at least c. 180 m, wide-spread open sea hypoxia developed around 1960 AD.

5.2 Chronology

Due to the problem of interpreting bulk radiocarbon ages in the Baltic Sea, it is hard to establish the exact ages for the formation of the laminated sediments in the beginning of the Littorina Sea. Comparing with other studies, the bulk age of hypoxia (laminated sediments) during this time (i.e. c. 8000-5000 cal. yr. BP.) is in accordance with previous studies (Zillén et al., 2008; Reinholdsson et al., in prep; Fig. 11). However, the age derived from the macrofossil remain (fish bone) at 248-249 cm in the gravity core suggests that the hypoxia during this period is centered around c. 4000 cal. yr. BP (Fig. 11). Unfortunately, no additional macrofossil remains were recorded in the sediment sequence (macrofossil remains is uncommon in Baltic Sea sediments) which would have allowed sedimentation rates to be calculated (similar as for the laminated period during the MCO).

However, if one uses the trend of the bulk radiocarbon ages during this time (the three lowermost bulk radiocarbon ages show a smooth trend, probably implying a generally stable sediment deposition rate; Fig. 10), a sediment accumulation rate can be calculated. Based on table 4, the sediment accumulation rate is 0.24 mm/yr between 215 cm and 259 cm, while is 0.27 mm/yr between 259 cm and 286 cm. Since the mass of macrofossil sample is within the accurate range of AMS dating (AMS is possible to carry out carbon dating on samples as small as 0.2 mg C), it should be reliable. Assuming no prominent sedimentation rate changes occurred during the lowermost laminated period, the timing of hypoxia is c. 5467 – 5902 cal. yr. BP.

Christiansen et al. (2002) proposed a sedimentation rate (0.23 mm/yr) in west part of eastern Gotland Basin based on high-resolution seismic recordings and correlation with long sediment cores, which demonstrates that the calculated sedimentation rate in this study is in range. In addition, Kortekaas et al. (2007) suggested a younger A/L transition age (6.5 ka) based on OSL age and macrofossil age in Arkona Basin, which supports the younger age of hypoxia in WGB.

In conclusion, more research needed to determine the age of hypoxia and the A/L transition in the Baltic Sea.

5.3 Origin of mineral magnetic signals

In order to detect the variation of magnetic concentration in the laminations, a scatter plot of χ VS SIRM is shown in figure 12A. The data have been divided into 3 groups based on a combination of sediment stratigraphy and time zone, the laminated group and poorly laminated group, non-laminated group and Ancylus Lake (AL) group, although the AL group is also belonging to non-laminated group. Low SIRM, but moderate X, plotting at the left have relatively high susceptibilities on account of paramagnetic contributions, and the ratios along the tilt slope represent the value of SIRM/χ above $10 * 10^3 Am^{-1}$ (Thompson and Oldfield, 1986), which corresponds to the samples within the major laminations in figure 6.

The distinct change around SIRM values of $1.0 * 10^{-3} Am^2 kg^{-1}$ suggested to use to delimit the "oxic-hypoxic (non-laminated-laminated)" zone. However, some data from the laminated group mix with non-laminated group. The laminated samples along the tilt slope correlate to the major laminated periods, but the mixed laminated samples present at the poorly laminated, minor laminated and the beginning or the ending of the major laminated periods (Fig.6), the reason for the distinction of these samples is unknown. In order to try to reveal these uncertainties, a hypothesis is proposed based on the study of Paasche and Løvlie (2011). In their study, the colonization of young lakes by magnetotactic bacteria (MTB) was investigated. MTB's are gram-negative aquatic microorganisms with ability to biomineralize single-domain magnetite in chains (Blakemore, 1975). MTB thrive at the oxic-anoxic transition zone, such as hypoxic zone, and are able to produce intercellular chains of pure magnetite in large quantities (Farina et al.,1990). Once they colonize a new habitat, they usually prevail, regardless of the changes in temperature, nutrients, salinity and pH, but varied by the local oxygen conditions (Lean and McCave, 1998). When they die, the chains of magnetite (or dispersed crystals) are incorporated into the sediments, which could be found in organic rich layers (Kim et al., 2005; Snowball, 1994).

The individual magnetite particles produced by MTBs are called magnetosomes and are frequently about 30-120 nm long (Devouard et al., 1998) and strictly within SD range of magnetite (Butler and Banerjee, 1975; Frankel et al., 1998). Since the ratio of ARM/SIRM (can be converted to χ_{ARM}/SIRM) can denote the mean distribution of magnetic grain size, it may be applied for the concentration of SD magnetite when the ratios $\geqq 0.1 \pm 0.01$ (Paasche and Løvlie, 2011). So they constructed a model of ratio ARM/SIRM against calibrated time to show the colonization process in their study sites. The ratio 0.1 is considered as the boundary between primary detrital magnetite and secondary biologically produced magnetite and is considered as the level of colonization.

A similar model is made in this study, but the SIRM replaces the calibrated time and the ratio of ARM/SIRM is converted to ratio χ_{ARM}/SIRM to take into account the DC bias field used to induce ARM (which can vary in different laboratories). ARM may

be varied by different measurements i.e. different measuring instruments. The solid line is the boundary when ARM/SIRM=0.1, and two dash lines represent the range of ARM/SIRM= 0.1±0.01. In addition, only the reliable data have been plotted (Fig.12B).

Comparing to the figure 12A, the samples over 1 * $10^{-3}Am^2kg^{-1}$of SIRM and above the lower dash line belong to those along the tilt slope, which show a result of colonization. Since the non-laminated group has been almost eliminated due to the unreliable ARM,

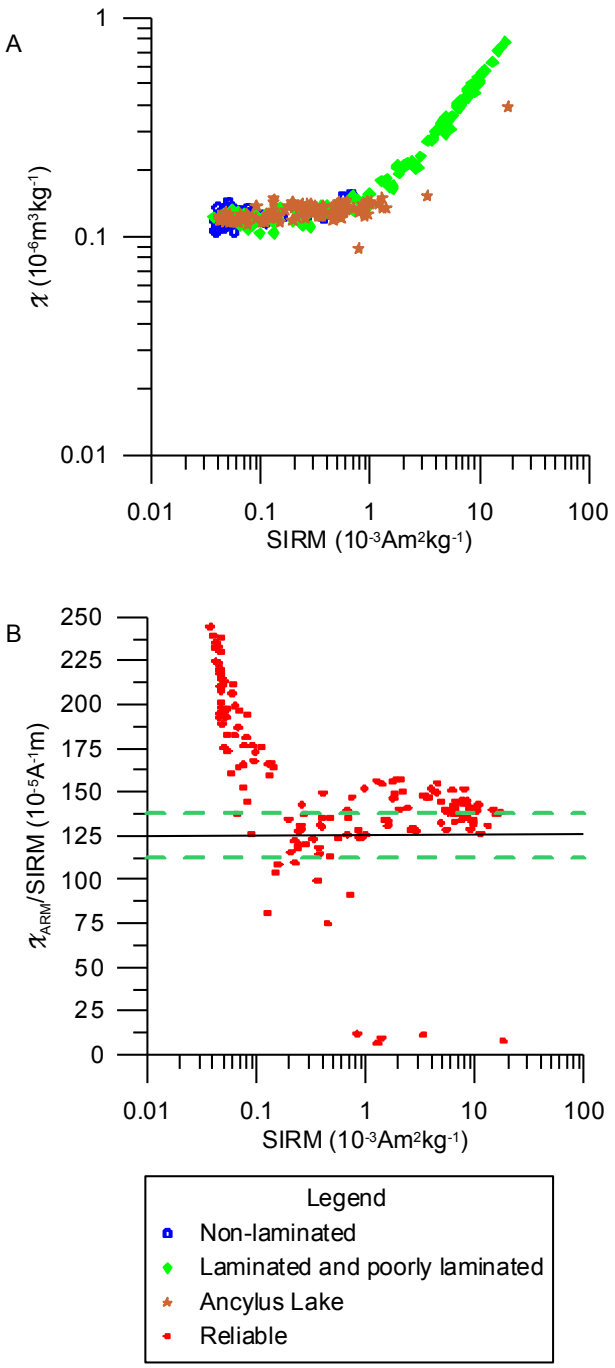

Fig. 12. A) Scatter plot of SIRM/χ with three groups, non-laminated, laminated and poorly laminated and Ancylus Lake; B) Scatter plot of χ_{ARM}/SIRM vs SIRM, with only reliable data in this study. The solid line represents the converted value when ARM/SIRM=0.1 and the two dash lines cover the converted range of ARM/SIRM=0.1±0.01.

the samples less than 1 * $10^{-3}Am^2kg^{-1}$ of SIRM are supposed to be the mixed laminated data, and most of them also indicate the result of colonization. However, those above 160 * $10^{-5}A^{-1}m$ of χ_{ARM}/SIRM are considered erroneous. The rest of the samples are counted to be colonized, except the samples below the lower dash line (Fig.12B).

The colonization by MTB's can be interpreted in two ways. The first interpretation assumes that MTB are very sensitive to the dissolved oxygen concentration and the population of MTB changes in an inverse proportion to the oxygen concentration, because they prefer low oxygen levels (Bazylinski, 1995). Once the oxygen concentration reaches their favorite level, they would thrive and colonize the sediments quickly. Otherwise, the population of MTB may stop growing or even die out. As shown in SIRM and χ (Fig.6), the values are generally high in major laminated periods, but quite low in homogeneous periods. During the poorly laminated and minor laminated periods, the values appear moderate. Secondly, perhaps the preservation condition is the key factor that determines the concentration of magnetosomes in the laminated sediments. MTB thrive at the oxic-anoxic transition zone (Farina et al.,1990), and they may favor the bottom water condition. However, the changes of oxygen concentration at the bottom result in different preservation conditions i.e. magnetite could be oxidized when the oxygen concentration is high (or reduced when very low), which causes the pattern of magnetic parameters (Fig.6).

In addition, comparing figure 8 to figure 12B, the range of susceptibility loss correlates to colonized range. As a result, the reason for susceptibility loss, which may be due to SD magnetite, may change to the loss of MTB. However, the available data only suggest that a fine grained ferrimagnet, which alters during storage in air, dominates the magnetic properties of the laminated units during the Littorina phase of the Baltic Sea. Its magnetic properties are different to greigite. The hypothesis set up is that this material is single-domain magnetite produced by MTB, which thrive in the hypoxic conditions. However, this hypothesis must be tested by positively identifying the individual magnetic grains using, for example, X-ray diffraction and quantitative geochemical analyses.

6 Conclusions

This study uses environmental proxy data to demonstrate that three major periods of basin-wide (western, eastern and northern Gotland Basins) hypoxia has been present in the Baltic Sea during the Littorina Sea stage.

The start of the modern hypoxic period is dated to 1960 and correlates to increased anthropogenic forcing (via eutrophication) known to have amplified hypoxia in the Baltic Sea and other coastal regions around the world. Based on lead pollution isochrones, the age of the second period of hypoxia started c. 1450±150 and ended c. 650±150 cal. yr. BP, which corresponds to the Medieval period when human impact and climate changes had a large effect on the

oxygen conditions in the basin.

According to radiocarbon measurements of bulk sediment samples, hypoxia in the beginning of the Littorina Sea occurred between c. 5000-8000 cal. yr BP (i.e. similar to previous studies). However, a single date based on radiocarbon measurements of a macrofossil remain (fish bone) suggests that hypoxia during this time period was much younger and centered around c. 4000 cal. yr BP. Based on the same date, the Ancylus/Littorina transition is dated to c. 6000 cal. yr. BP, which adds further information to the discussion about the age of the "modern" Baltic Sea.

The reason for the magnetic peaks in laminations remains to be determined. The peaks are caused by high concentration of fine grained ferrimagnetic minerals that need to be positively identified using other techniques.

7 Acknowledgements

This work is a contribution from the BONUS project HYPER. This work was also supported by a grant from Kungl. Fysiografiska Sällskapet I Lund. I wish to express my sincere gratitude to my supervisors Lovisa Zillén, Ian Snowball, Conny Lenz and Maja Reinholdsson for their help during the entire thesis work, especially for Lovisa's great help on the later versions of the manuscript. I also want to acknowledge Bryan Lougheed for his comments during the thesis writing and thank Åsa Wallen for her help during the practical work.

8 References

Andrén, T., Björck, J. and Johnsen, S. (1999), Correlation of Swedish glacial varves with the Greenland (GRIP) oxygen isotope record. *Journal of Quaternary Science 14*(4), pp. 361- 371.

Andrén, T. (2003a), Baltiska Issjön – eller hur det började, *Havsutsikt, 1*, pp. 4-5.

Andrén, T. (2003b), Yoldiahavet – en viktig parentes, *Havsutsikt, 2*, pp. 6-7.

Andrén, T. (2003c), Ancylussjön – fortfarande ett mysterium, *Havsutsikt, 3*, pp. 8-9.

Andrén, T. (2004), Littorinahavet – en salt historia, *Havsutsikt, 1*, pp. 8-9.

Axe, P. (2004), Hydrography and Oxygen in the Deep Basins, SMHI, Sweden.

Bazylinski, D. A. (1995), Controlled biomineralization of magnetic minerals by magnetotactic bacteria, *Chemical Geology 132*, pp. 191–198.

Bengtsson, L. and M. Enell (1986), Chemical analysis, In: *Handbook of Holocene Palaeoecology and Palaeohydrology*, Berglund, B. E. (ed.), pp. 423-451, John Wiley & Sons Ldt., Chichester.

Berglund, B. E., Sandgren, P., Barnekow, L., Hannon, G., Jiang, H., Skog, G. and S.-Y, Yu (2005), Early Holocene history of the Baltic Sea, as reflected in coastal sediments in Blekinge, southeastern Sweden, *Quat. Int., 130*, pp. 111-139.

Bianchi, T. S., Engelhaupt, E., Westman, P., Andrén, T., Rolff, C. and R. Elmgren (2000): Cyanobacterial blooms in the Baltic Sea: Natural or human induced?, *Limnology and Oceanography 4*(3), pp. 716-726.

Björck, S. (1995), A review of the history of the Baltic Sea, 13.0-8.0 ka BP, *Quaternary International, 27*, pp. 19-40.

Björck, S. (2008), The late Quaternary development of the Baltic Sea, In: *Assessment of climate change for the Baltic Sea Basin*, BACC Author Team, pp. 398-407, Springer-Verlag Berlin and Heidelberg GmbH & Co. KG. K, Berlin, Germany.

Björck, S., Andrén, T. And J. B. Jensen (2008), An attempt to resolve the partly conflicting data and ideas on the Ancylus-Littorina transition, *Polish Geological Institute Special Papers, 23*, pp21-25.

Blakemore, R. (1975), Magnetotactic Bacterina, *Science 190* (4212), pp. 377–379.

Bradshaw, E. G., Rasmussen, P., Nielsen, H., and N. J. Andersen (2005), Mid- to Late-Holocene land change and lake development at Dallund Sø, Denmark: trends in lake primary production as reflected by algal and macrophyte remains, *The Holocene, 15*(8), pp. 1130– 1142.

Bronk, R. C. (2009), Bayesian analysis of radiocar bon dates, *Radiocarbon, 51*(1), pp. 337-360.

Brännvall, M. –L., Bindler, R., Emteryd, O. and I. Renberg (2001), Four thousand years of atmospheric lead pollution in northern Europe: a summary from Swedish lake sediments, *Journal of Paleolimnology 25*, pp. 421–435.

Butler, R.F., and S. K. Banerjee (1975), Theoretical single-domain grain-size range in magnetite and titanomagnetite, *Journal of Geophysical Research, 80*, pp. 4049–4058.

Christiansen, C., Kunzendorf, H., Emeis, K.-C., Endler, R., Struck, U., Neumann, T. and V. Sivkov (2002), Temporal and spatial sedimentation rate variabilities in the eastern Gotland Basin, the Baltic Sea, *Boreas, Vol. 31*, pp. 65–74.

Conley, D.J., Humborg, C., Rahm, L., Savchuk, O.P., and F. Wulff (2002), Hypoxia in the Baltic Sea and Basin-Scale changes in phosphorous and biogeochemistry, *Environmental Science and Technology, 36*, 5315–5320.

Conley, D.J., Bonsdorff, E., Carstensen, J., Destouni, G., Gustafsson, B. G., Hansson, L-A., Rabalais, N. N., Voss, M., and L. Zillén (2009), Tackling Hypoxia in the Baltic Sea: Is Engineering a Solution? *Environ. Sci. Technol, 43*(10), pp. 3407-3411.

Conley, D. J., Björck, S., Bonsdorff, E., Carstensen, J., Destouni, G., Gustafsson, B. G., Hietanen, S., Kortekaas, M., Kuosa, H., Meier, H. E. M., Müller-Karulis, B., Nordberg, K., Norkko, A., Nürnberg, G., Pitkänen, H., Rabalais, N. N., Rosenberg, R., Savchuk, O. P., Slomp, C. P., Voss, M., Wulff, F. and L. Zillén (2009), Hypoxia-Related Processes in the Baltic Sea, *Environ. Sci. Technol. 43*(10), pp. 3412-3420.

Dean, W. E. Jr. (1974), Determination of carbonate and organic matter in calcareous sediments and sedimentary rocks by loss on ignition: Comparison with other methods, *J. Sed. Petrol., 44*, pp. 242-248.

Devouard, B., Posfai, M., Hua, X., Bazylinski, D.A., Frankel, R.B. and P. R. Buseck, (1998), Magnetite from magnetotactic acteria: Size distributions and twinning, *American Mineralogist, 83*, pp. 1387–1398.

Diaz, R. J. and R. Rosenberg (1995), Marine benthic hypoxia - review of ecological effects and behavioral responses on macrofauna, *Oceanography and Marine Biology, Annual Review. 33*, pp. 245-303.

Diaz, R.J. and R. Rosenberg (2008), Spreading dead zones and consequences for marine ecosystems, *Science 321*, pp. 926-928.

Farina, M., Esquivel, D.M.S. and H. Debarros (1990), Magnetic iron-sulfur crystals from a magnetotactic microorganism, *Nature, 343*, pp. 256–258.

Feistel, R., Nausch, G., Mohrholz, V., Łysiak-Pastuszak, E., Seifert, T., Matthäus, W., Krüger, S. and I. S. Hansen (2003c), Warm waters of summer 2002 in the deep Baltic Proper, *Oceanologia 45*(4), 571-592.

Feistel, R., Nausch, G., Matthäus, W., Lysiak-Pastuszak, E., Seifert, T., Schested H. I., Mohrholz, V., Krüger, S., Bush, E. and E. Hagen (2004a), *Background data to the exceptionally warm inflow into the Baltic Sea in the summer 2002*, pp. 58, Meereswissenschaftliche Berichte 58, Institute for Baltic Sea Research, Warnemunde, Germany.

Frankel, R.B., Zhang, J.P., and D. A. Bazylinski (1998), Single magnetic domains in magnetotactic bacteria, *Journal of Geophysical Research, 103*(B12), pp. 30,601–30,604.

Gustafsson, B. G. and P. Westman (2002), On the causes for salinity ariations in the Baltic Sea during the last 8500 years, *PALEOCEANOGRAPHY, 17*(3), pp. 1-14.

Heiri, O., Lotter, A. F. and G. Lemcke (2001), Loss on ignition as a method for estimating organic and carbonate content in sediments: reproducibility and comparability of results, *Journal of Paleolimnology, 25*, pp. 101-110.

Håkansson, B., Axe, P. and M. Hansson (2005), Swedish National Report on Eutrophication of the Western Gotland Basin. Internal Report, pp. 8, HELCOM EUTRO Project.

Jonsson, P., Carman, R. and F. Wulff (1990), Laminated Sediments in the Baltic: A Tool for Evaluating Nutrient Mass Balances, *Ambio 19* (3), pp. 152-158.

Kim, B.Y., Kodama, K.P., and R. E. Moeller (2005), Bacterial magnetite produced in water column dominates lake sediment mineral magnetism: Lake Ely, *Geophysical Journal International, 163*, pp. 26–37.

Komeili, A., Li, Z. and D. K. Newman (2006), Magnetosomes Are Cell Membrane Invaginations Organized by the Actin-Like Protein MamK, *Science, 311*, pp. 242-245.

Kortekaas, M., Murray, A. S., Sandgren, P. and S. Björck (2007), OSL chronology for a sediment core from the southern Baltic Sea: A continuous sedimentation record since deglaciation, *Quaternary Geochronology v. 2*, pp. 95-101.

Lean, C.M.B. and I. N. McCave (1998), Glacial to interglacial mineral magnetic and palaeoceanographic changes at Chatham Rise, SW Pacifi c Ocean, *Earth and Planetary Science Letters, v. 163*, pp. 247–260.

Lemke, W. (1998), *Sedimentation und paläogeographische Entwicklung im westlichen Ostseeraum (Mecklenburger Bucht bis Arkonabecken) vom Ende der Weichselvereisung bis zur Littorina-transgression*, Meereswissenschaftliche Berichte 31, Institute for Baltic Sea Research, Warnemunde, Germany.

Lowe, J. J. and M. J. C., Walker, (1997), *Reconstructing Quaternary Environments*, pp. 446, monografiga, Edinburgh.

Maher, B. A. and R. Thompson (1999), *Quaternary Climate, Environments and Magnetism*, pp. 402, Cambridge University Press, Cambridge.

Matthäus, W. and H. Schinke, (1999), The influence of river runoff on deep water conditions of the Baltic Sea, *Hydrobiologia, 393*, pp. 1-10.

Matthäus, W. (2006), *The history of investigation of salt water inflow into the Baltic Sea — from the early beginning to recent results*, Marine Science Reports, 65, Baltic Sea Research Institute, Warnemunde, Germany.

Matthäus, W., Nehring, D., Feistel, R., Nausch, G., Mohrholz, V. and H.-U. Lass (2008), The inflow of highly saline water into the Baltic Sea, In: *State and evolution of the Baltic Sea 1952-2005, a detailed 50-year survey of meteorology and climate, physics, chemistry, biology, and marine environment*, Feistel, R., Nausch, G. and N. Wasmund (ed.), John Wiley & Sons, Inc., Hoboken, New Jersey.

Paasche, Ø. and R. Løvlie (2010), Synchronized postglacial colonization by magnetotactic bacteria, *Geology, 39*(1), pp. 75-78.

Plastino, W., Kaihola, L., Bartolomei, P. and F. Bella (2001), Cosmic Background Reduction In The Radiocarbon Measurement By Scintillation Spectrometry At The Underground Laboratory Of Gran Sasso, *Radiocarbon, 43*(2A), pp. 157–161.

Reinholdsson, M., Snowball, I. F., Zillén, L. and D. J., Conley, On the origin of fine-grained magnetic mineral (magnetite?) in laminated Baltic Sea sediments and implications for past environmental variability, in prep.

Renberg, I., Brännvall, M-L., Bindler, R. And O. Emteryd (2000), Atmospheric Lead Pollution History during Four Millennia (2000 BC to 2000 AD) in Sweden, *Ambio, vol. 29*(3), pp. 150-156.

Renberg, I., Bindler, R., Bradshaw, E., Emteryd, O. and S. McGowan (2001), Sediment evidence of early eutrophication and heavy metal pollution in Lake Mälaren, Central Sweden, *Ambio, 30*, pp. 496–502.

Rößler, D., Moros, M. and W. Lemke (2010), The Littorina transgression in the southwestern Baltic Sea: new insights based on proxy methods and radiocarbon dating of sediment cores, *Boreas, 40*, pp 231-241.

Schinke, H. (1996), *Zu den Ursachen von Salzwassereinbrüchen in die Ostsee*, pp. 1-137, Meereswissenschaftliche Berichte 12, Institute for Baltic Sea Research, Warnemunde, Germany.

Schinke, H and W. Matthäus (1998), On the cause of major Baltic inflows – an analysis of long time series, *Continental Shelf Research, 18*, pp. 67-97.

Snowball, I. F. (1994), Bacterial magnetite and the magnetic properties of sediments in a Swedish lake, *Earth and Planetary Science Letters, 126*, pp. 129-142.

Snowball, I. F., Zillén, L. and P. Sandgren (2002), Bacterial magnetite in Swedish varved lake-sediments: A potential bio-marker of environmental change, *Quaternary International, v. 88*, pp. 13–19.

Snowball, I. F., Muscheler, R., Zillén, L., Sandgren, P., Stanton, T. and K. Ljung (2010), Radiocarbon wiggle-matching of Swedish varves reveals asynchronous climate changes around the 8.2 kyr cold event. *Boreas, 39*, pp. 720-733.

Szaron, J. (2001), Expeditionsrapport från U/F argos cruise report from R/V argos, SMHI, Sweden.

Thompson, R. and F. Oldfield (1986), *Environmental magnetism*, pp. 227, Allen and Unwin Ltd, London.

Vahtera, E., Conley, D., Gustafsson, BG., Kuosa, H. and others (2007), Internal ecosystem feedbacks enhance nitrogen fixing cyanobacteria blooms and complicate management in the Baltic Sea, *Ambio, 36,* pp. 186-194.

Walden, J., Oldfield, F. and J. Smith (1999), E*nvironmental magnetism a practical guide*, Technical Guide, No. 6, Quaternary Research Association, London.

Zillén, L., Conley, D. J., Andern, T., Andren, E. and S. Björck (2008), Past occurrences of hypoxia in the Baltic Sea and the role of climate variability, environmental change and human impact, *Earth-Science Reviews, 91*, pp. 77-92.

Zillén, L. and D. J. Conley (2010), Hypoxia and cyanobacteria blooms- are they really natural features of the late Holocene history of the Baltic Sea?, *Biogeosciences, 7*, 2567-2580.

Zillén, L., Lenz, C. and T. Jilbert (2011), Stable lead (Pb) isotopes and concentrations – A useful independent dating tool for Baltic Sea sediments, *Quaternary Geochronology*, In press.

Österblom, H., Hansson, S., Larsson, U., Hjerne, O., Wulff, F., Elmgren, R. and C. Folke (2007), Human-induced thropic cascades and ecological regime shifts in the Baltic Sea, *Ecosystems, 10* (6), pp. 1–13.

Tidigare skrifter i serien ”Examensarbeten i Geologi vid Lunds Universitet”:

245. Wollein Waldetoft, Kristofer, 2009: Svekofennisk granit från olika metamorfa miljöer. (15 hskp)
246. Månsby, Urban, 2009: Late Cretaceous coprolites from the Kristianstad Basin, southern Sweden. (15 hskp)
247. MacGimpsey, I., 2008: Petroleum Geology of the Barents Sea. (15 hskp)
248. Jäckel, O., 2009: Comparison between two sediment X-ray Fluorescence records of the Late Holocene from Disko Bugt, West Greenland; Paleoclimatic and methodological implications. (45 hskp)
249. Andersen, Christine, 2009: The mineral composition of the Burkland Cu-sulphide deposit at Zinkgruvan, Sweden – a supplementary study. (15 hskp)
250. Riebe, My, 2009: Spinel group minerals in carbonaceous and ordinary chondrites. (15 hskp)
251. Nilsson, Filip, 2009: Föroreningsspridning och geologi vid Filborna i Helsingborg. (30 hskp)
252. Peetz, Romina, 2009: A geochemical characterization of the lower part of the Miocene shield-building lavas on Gran Canaria. (45 hskp)
253. Åkesson, Maria, 2010: Mass movements as contamination carriers in surface water systems – Swedish experiences and risks.
254. Löfroth, Elin, 2010: A Greenland ice core perspective on the dating of the Late Bronze Age Santorini eruption. (45 hskp)
255. Ellingsgaard, Óluva, 2009: Formation Evaluation of Interlava Volcaniclastic Rocks from the Faroe Islands and the Faroe-Shetland Basin. (45 hskp)
256. Arvidsson, Kristina, 2010: Geophysical and hydrogeological survey in a part of the Nhandugue River valley, Gorongosa National Park, Mozambique. (45 hskp)
257. Gren, Johan, 2010: Osteo-histology of Mesozoic marine tetrapods – implications for longevity, growth strategies and growth rates. (15 hskp)
258. Syversen, Fredrikke, 2010: Late Jurassic deposits in the Troll field. (15 hskp)
259. Andersson, Pontus, 2010: Hydrogeological investigation for the PEGASUS project, southern Skåne, Sweden. (30 hskp)
260. Noor, Amir, 2010: Upper Ordovician through lowermost Silurian stratigraphy and facies of the Borenshult-1 core, Östergötland, Sweden. (45 hskp)
261. Lewerentz, Alexander, 2010: On the occurrence of baddeleyite in zircon in silica-saturated rocks. (15 hskp)
262. Eriksson, Magnus, 2010: The Ordovician Orthoceratite Limestone and the Blommiga Bladet hardground complex at Horns Udde, Öland. (15 hskp)
263. Lindskog, Anders, 2010: From red to grey and back again: A detailed study of the lower Kundan (Middle Ordovician) ‘Täljsten’ interval and its enclosing strata in Västergötland, Sweden. (15 hskp)
264. Rääf, Rebecka, 2010: Changes in beyrichiid ostracode faunas during the Late Silurian Lau Event on Gotland, Sweden. (30 hskp)
265. Petersson, Andreas, 2010: Zircon U-Pb, Hf and O isotope constraints on the growth versus recycling of continental crust in the Grenville orogen, Ohio, USA. (45 hskp)
266. Stenberg, Li, 2010: Geophysical and hydrogeological survey in a part of the Nhandugue River valley, Gorongosa National Park, Mozambique – Area 1 and 2. (45 hskp)
267. Andersen, Christine, 2010: Controls of seafloor depth on hydrothermal vent temperatures - prediction, observation & 2D finite element modeling. (45 hskp)
268. März, Nadine, 2010: When did the Kalahari craton form? Constraints from baddeleyite U-Pb geochronology and geo-chemistry of mafic intrusions in the Kaapvaal and Zimbabwe cratons. (45 hp)
269. Dyck, Brendan, 2010: Metamorphic rocks in a section across a Svecnorwegian eclogite-bearing deformation zone in Halland: characteristics and regional context. (15 hp)
270. McGimpsey, Ian, 2010: Petrology and lithogeochemistry of the host rocks to the Nautanen Cu-Au deposit, Gällivare area, northern Sweden. (45 hp)
271. Ulmius, Jan, 2010: Microspherules from the lowermost Ordovician in Scania, Sweden – affinity and taphonomy. (15 hp)
272. Andersson, Josefin, Hybertsen, Frida, 2010: Geologi i Helsingborgs kommun – en geoturistkarta med beskrivning. (15 hp)

273. Barth, Kilian, 2011: Late Weichselian glacial and geomorphological reconstruction of South-Western Scania, Sweden. (45 hp)
274. Mashramah, Yaser, 2011: Maturity of kerogen, petroleum generation and the application of fossils and organic matter for paleotemperature measurements. (45 hp)
275. Vang, Ina, 2011: Amphibolites, structures and metamorphism on Flekkerøy, south Norway. (45 hp)
276. Lindvall, Hanna, 2011: A multi-proxy study of a peat sequence on Nightingale Island, South Atlantic. (45 hp)
277. Bjerg, Benjamin, 2011: Metodik för att förhindra metanemissioner från avfallsdeponier, tillämpad vid Albäcksdeponin, Trelleborg. (30 hp)
278. Pettersson, Hanna, 2011: El Hicha – en studie av saltstäppssediment. (15 hskp)
279. Dyck, Brendan, 2011: A key fold structure within a Sveconorwegian eclogite-bearing deformation zone in Halland, south-western Sweden: geometry and tectonic implications. (45 hp)
280. Hansson, Anton, 2011: Torvstratigrafisk studie av en trädstamshorisont i Viss mosse, centrala Skåne kring 4 000 - 3 000 cal BP med avseende på klimat- och vattenståndsförändringar. (15 hp)
281. Åkesson, Christine, 2011: Vegetationsutvecklingen i nordvästra Europa under Eem och Weichsel, samt en fallstudie av en submorän, organisk avlagring i Bellinga stenbrott, Skåne. (15 hp)
282. Silveira, Eduardo M., 2011: First precise U-Pb ages of mafic dykes from the São Francisco Craton. (45 hp)
283. Holm, Johanna, 2011**:** Geofysisk utvärdering av grundvattenskydd mellan väg 11 och Vombs vattenverk. (15 hp)
284. Löfgren, Anneli, 2011: Undersökning av geofysiska metoders användbarhet vid kontroll av den omättade zonen i en infiltrationsdamm vid Vombverket. (15 hp)
285. Grenholm, Mikael, 2011: Petrology of Birimian granitoids in southern Ghana - petrography and petrogenesis. (15 hp)
286. Thorbergsson, Gunnlaugur, 2011: A sedimentological study on the formation of a hummocky moraine at Törnåkra in Småland, southern Sweden. (45 hp)
287. Lindskog, Anders, 2011: A Russian record of a Middle Ordovician meteorite shower: Extraterrestrial chromite in Volkhovian-Kundan (lower Darriwilian) strata at Lynna River, St. Petersburg region. (45 hp)
288. Gren, Johan, 2011: Dental histology of Cretaceous mosasaurs (Reptilia, Squamata): incremental growth lines in dentine and implications for tooth replacement. (45 hp)
289. Cederberg, Julia, 2011: U-Pb baddelyit dateringar av basiska gångar längs Romeleåsen i Skåne och deras påverkan av plastisk deformation i Protoginzonen (15 hp)
290. Ning, Wenxing, 2011: Testing the hypothesis of a link between Earth's magnetic field and climate change: a case study from southern Sweden focusing on the 1st millennium BC. (45 hp)
291. Holm Östergaard, Sören, 2011: Hydrogeology and groundwater regime of the Stanford Aquifer, South Africa. (45 hp)
292. Tebi, Magnus Asiboh, 2011: Metamorphosed and partially molten hydrothermal alteration zones of the Akulleq glacier area, Paamiut gold province, South-West Greenland. (45 hp)
293. 293. Lewerentz, Alexander, 2011: Experimental zircon alteration and baddeleyite formation in silica saturated systems: implications for dating hydrothermal events. (45 hp)
294. Flodhammar, Ingrid, 2011: Lövestads åsar: En isälvsavlagring bildad vid inlandsisens kant i Weichsels slutskede. (15 hp)
295. Liu, Tianzhuo, 2012: Exploring long-term trends in hypoxia (oxygen depletion) in Western Gotland Basin, the Baltic Sea. (45 hp)

LUNDS UNIVERSITET

Geologiska institutionen
Lunds universitet
Sölvegatan 12, 223 62 Lund